Overall Design and Experimental Verification of Piezoelectric Smart Structures for Vibration and Noise Control

Ulrich Gabbert

Otto-von-Guericke University of Magdeburg
Institute of Mechanics
Computational Mechanics

Tel. +49-391-6718608, Fax +49-391-67-12439
E-Mail: ulrich.gabbert@mb.uni-magdeburg.de

Workshop on "Direct and Inverse Problems in Piezoelectricty"
Johann Radon Institute Linz
6. – 7. October 2005

Contents

Objectives of the Smart Systems Group at the Mechanics Institute

- Vibration and noise control, shape control
- Modelling, simulation, overall design tools
- Experimental verification (hardware-in-the-loop realization) and applications

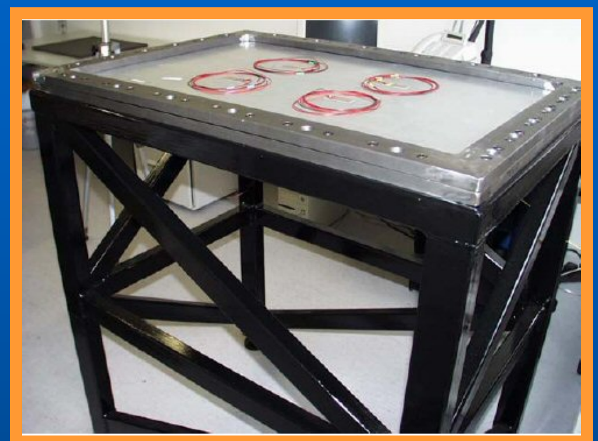

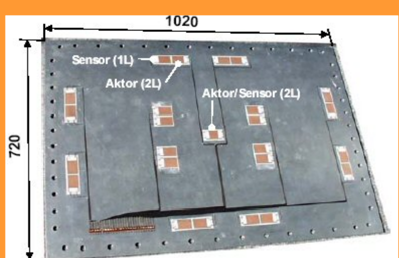

Vibration and noise suppression under different operation conditions

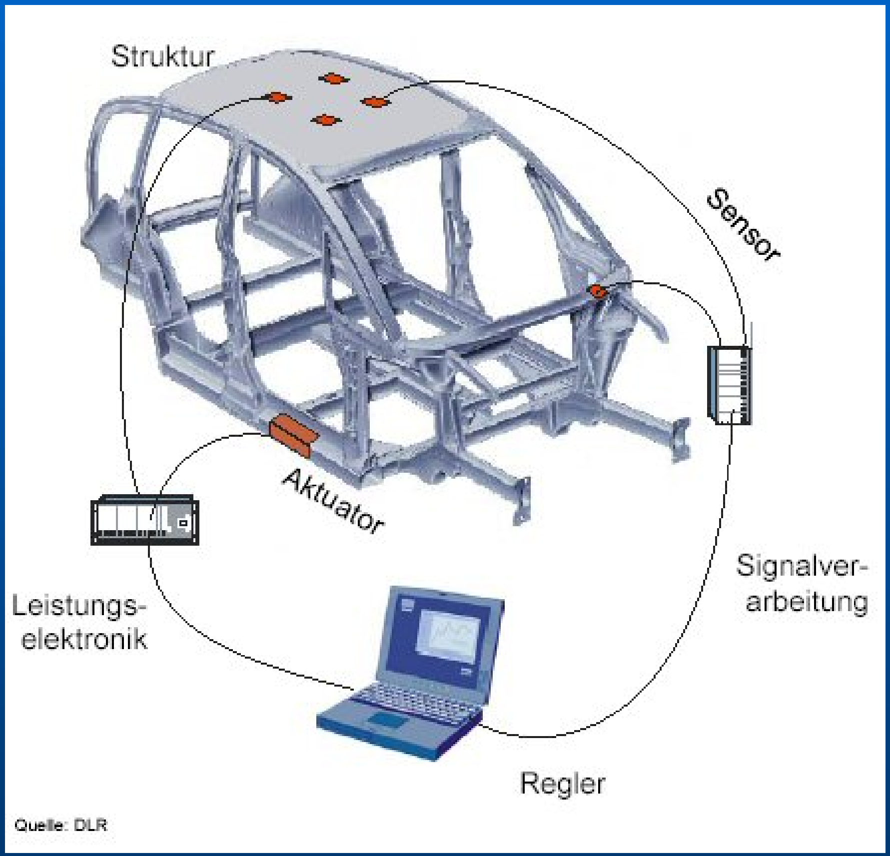

Virtual Systems Design

1. Selection of appropriate actuators and sensors
2. Optimal placement of actuators and sensors at the structure
3. Design of the controller
4. Overall virtual simulation of the system
5. Optimisation of the system
6. Hardware-in-the-loop experiments

Tools for the virtual development process

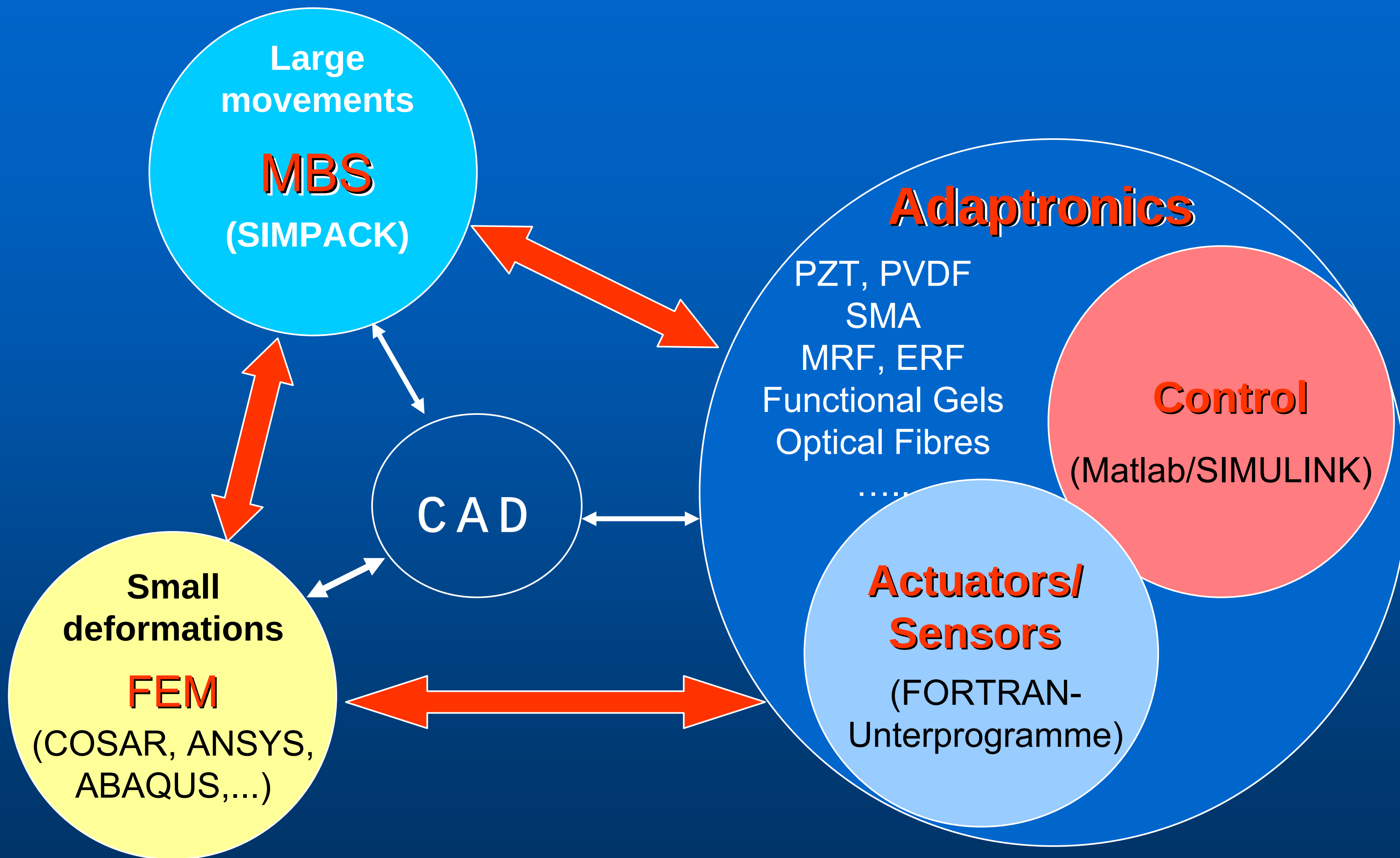

Constitutive Equations

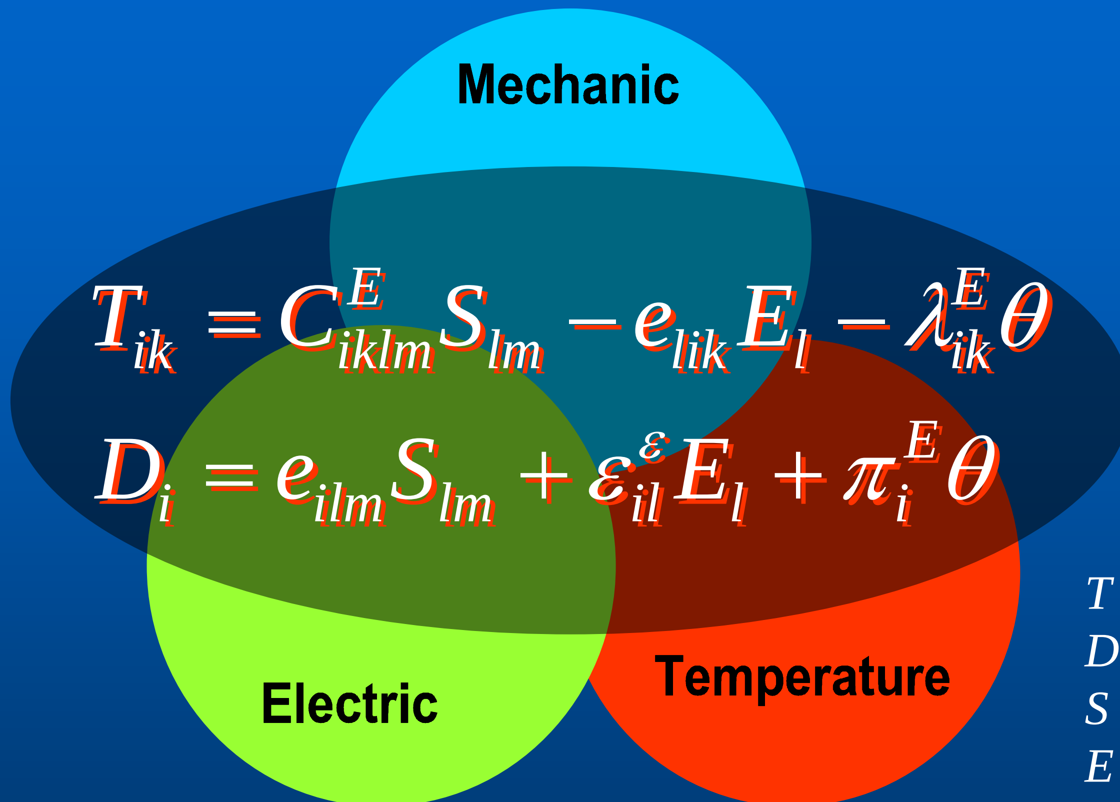

$$T_{ik} = C^{E}_{iklm} S_{lm} - e_{lik} E_{l} - \lambda^{E}_{ik} \theta$$

$$D_{i} = e_{ilm} S_{lm} + \varepsilon^{\varepsilon}_{il} E_{l} + \pi^{E}_{i} \theta$$

T – stresses,
D – el. displacements
S – strains,
E – electric field

Görnand, A., Gabbert, U.: Finite element analysis of thermopiezoelectric smart structures. Acta Mechanica 154, 129-140 (2002).

3D constitutive equations

$$\mathbf{C}=\begin{bmatrix} c_{11} & c_{12} & c_{13} & 0 & 0 & 0 \\ & c_{11} & c_{13} & 0 & 0 & 0 \\ & & c_{33} & 0 & 0 & 0 \\ & & & c_{66} & 0 & 0 \\ & symm. & & & c_{44} & 0 \\ & & & & & c_{44} \end{bmatrix} \quad \mathbf{e} = \begin{bmatrix} 0 & 0 & e_{31} \\ 0 & 0 & e_{31} \\ 0 & 0 & e_{33} \\ 0 & e_{15} & 0 \\ e_{15} & 0 & 0 \end{bmatrix} \quad \boldsymbol{\varepsilon}=\begin{bmatrix} \varepsilon_{11} & 0 & 0 \\ & \varepsilon_{11} & 0 \\ symm. & & \varepsilon_{33} \end{bmatrix}$$

Basics of thermo-electro-mechanics

Balance equations

$$\operatorname{div}\boldsymbol{\sigma} + \rho\bar{\mathbf{b}} - \rho\frac{\partial^2 \mathbf{u}}{\partial t^2} = 0$$

$$\operatorname{div}\mathbf{D} = 0$$

$$\operatorname{div}\mathbf{q} - \rho r + \Theta\rho\dot{\eta} = 0$$

Weak form of the balance equations

$$\int_V (\operatorname{div}\boldsymbol{\sigma} + \rho\bar{\mathbf{b}} - \rho\frac{\partial^2 \mathbf{u}}{\partial t^2})\delta\mathbf{u}\, dV + \int_V (\operatorname{div}\mathbf{D})\delta\phi\, dV + \int_V (\operatorname{div}\mathbf{q} - \rho r + \Theta\rho\dot{\eta})\delta\vartheta\, dV + \ldots BCs\ldots = 0$$

Finite element approximation

Approximation of the unknown fields

Displacements: $u_i = \sum_{L=1}^{M^{(me)}} N_L^{(me)} u_{iL}$ Electric potential: $\phi = \sum_{L=1}^{M^{(el)}} N_L^{(el)} \phi_L$

Temperature: $\vartheta = \sum_{L=1}^{M^{(th)}} N_L^{(th)} \vartheta_L$

Semi-discrete form of the equations of motion

$$\begin{bmatrix} \mathbf{M}_{uu} & \mathbf{0} & \mathbf{0} \\ \mathbf{0} & \mathbf{0} & \mathbf{0} \\ \mathbf{0} & \mathbf{0} & \mathbf{0} \end{bmatrix} \begin{bmatrix} \ddot{\mathbf{u}} \\ \ddot{\boldsymbol{\phi}} \\ \ddot{\vartheta} \end{bmatrix} + \begin{bmatrix} \mathbf{R}_{uu} & \mathbf{0} & \mathbf{0} \\ \mathbf{0} & \mathbf{0} & \mathbf{0} \\ \Theta\mathbf{K}_{\vartheta u} & -\Theta\mathbf{K}_{\vartheta\phi} & \mathbf{H}_{\vartheta\vartheta} \end{bmatrix} \begin{bmatrix} \dot{\mathbf{u}} \\ \dot{\boldsymbol{\phi}} \\ \dot{\vartheta} \end{bmatrix} + \begin{bmatrix} \mathbf{K}_{uu} & \mathbf{K}_{u\phi} & -\mathbf{K}_{u\vartheta} \\ \mathbf{K}_{\phi u} & -\mathbf{K}_{\phi\phi} & \mathbf{K}_{\phi\vartheta} \\ \mathbf{0} & \mathbf{0} & \mathbf{K}_{\vartheta\vartheta} \end{bmatrix} \begin{bmatrix} \mathbf{u} \\ \boldsymbol{\phi} \\ \vartheta \end{bmatrix} = \begin{bmatrix} f_u \\ f_\phi \\ f_\vartheta \end{bmatrix}$$

Coupling with the acoustic field

The basis is the linear acoustic wave equation (small perturbations related to an ambient reference state)

$$\Delta p = \frac{1}{c^2}\ddot{p}$$

With the velocity potential Φ, which is a scalar field related to the velocity as $\mathbf{v} = -\mathbf{D}_a \Phi$ of the fluid particles the pressure can be written as $p = \rho_0 \dot{\Phi}$. This results in

$$\Delta \Phi = \frac{1}{c^2}\ddot{\Phi}$$

The weak form of the acoustic wave equation results in

$$\chi = -\frac{1}{c^2}\int_f \delta\Phi\ddot{\Phi}\, dV - \frac{\rho_0}{\overline{Z}}\int_{O_Z} \delta\Phi\dot{\Phi}\, dO - \int_{V_i} \delta\Phi\, \mathbf{D}_a^T \mathbf{D}_a\, \Phi\, dV - \int_{O_v} \delta\Phi \overline{v}_n dO \mathbf{D}_a^T\, \mathbf{D}_a^T \Phi = 0$$

$$\mathbf{D}_a^T = \begin{bmatrix} \frac{\partial}{\partial x} & \frac{\partial}{\partial y} & \frac{\partial}{\partial z} \end{bmatrix}$$

Vibro-acoustic coupling for smart structures

$$\begin{bmatrix} \mathbf{M}_{ww} & \mathbf{0} & \mathbf{0} \\ \mathbf{0} & \mathbf{0} & \mathbf{0} \\ \mathbf{0} & \mathbf{0} & -\rho_0 \mathbf{M}_a \end{bmatrix} \begin{bmatrix} \ddot{\mathbf{w}} \\ \ddot{\boldsymbol{\varphi}} \\ \ddot{\boldsymbol{\Phi}} \end{bmatrix} + \begin{bmatrix} \mathbf{C}_{ww} & \mathbf{0} & -\mathbf{C}_{wc} \\ \mathbf{0} & \mathbf{0} & \mathbf{0} \\ -\mathbf{C}_{wc}^T & \mathbf{0} & -\rho_0(\mathbf{C}_a + \mathbf{C}_I) \end{bmatrix} \begin{bmatrix} \dot{\mathbf{w}} \\ \dot{\boldsymbol{\varphi}} \\ \dot{\boldsymbol{\Phi}} \end{bmatrix} +$$

$$\begin{bmatrix} \mathbf{K}_{ww} & \mathbf{K}_{w\varphi} & \mathbf{0} \\ \mathbf{K}_{w\varphi}^T & -\mathbf{K}_{\varphi\varphi} & \mathbf{0} \\ \mathbf{0} & \mathbf{0} & -\rho_0(\mathbf{K}_a + \mathbf{K}_I \end{bmatrix} \begin{bmatrix} \mathbf{w} \\ \boldsymbol{\varphi} \\ \boldsymbol{\Phi} \end{bmatrix} = \begin{bmatrix} \mathbf{f}_w \\ \mathbf{f}\varphi \\ -\rho_0 \mathbf{f}_a \end{bmatrix}$$

The velocity of the vibrating structure acts as a acoustic load of the fluid
The normal velocity of the structure can be expressed as $\dot{u}_n = \mathbf{n}^T \mathbf{N}_w \dot{\mathbf{w}}$

$$\mathbf{f}_{ac} = -\int_{O_S^{(e)}} \mathbf{N}_a^T \mathbf{n}^T \mathbf{N}_w dO \, \dot{\mathbf{w}} = \frac{1}{\rho_0} \mathbf{C}_{wc}^T \dot{\mathbf{w}}$$

With an additional load term due to the fluid pressure

$$\mathbf{f}_{wc} = \int_{O_S^{(e)}} \mathbf{N}_w^T \mathbf{n} p dO = \rho_0 \int_{O_S^{(e)}} \mathbf{N}_w^T \mathbf{n} \mathbf{N}_a dO \, \dot{\boldsymbol{\Phi}} = \mathbf{C}_{wc} \dot{\boldsymbol{\Phi}}$$

Finite element software for piezoelectric smart systems

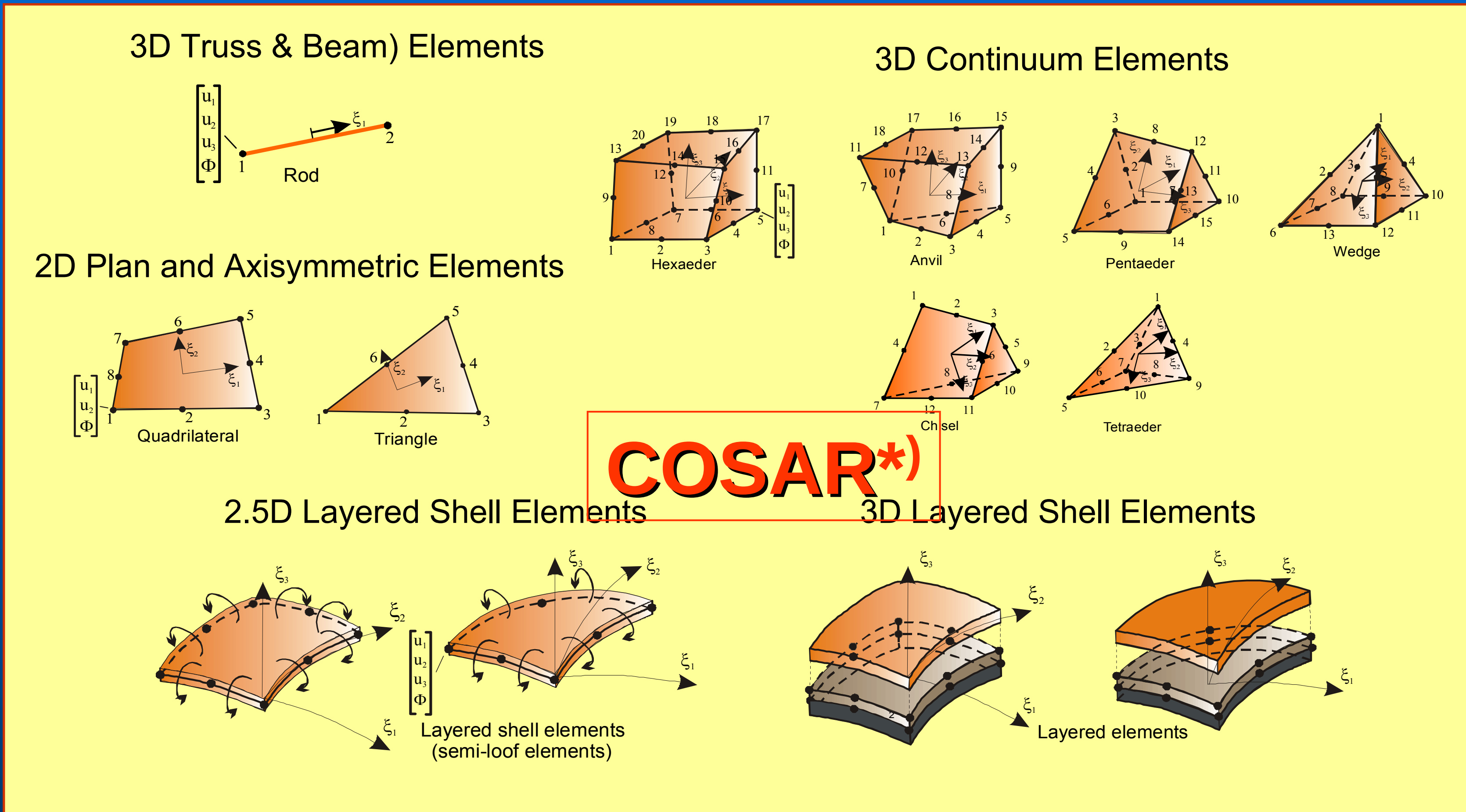

*) siehe www.femcos.de

Linz, 7. Oktober 2005

Modelling piezoelectric fibres

Piezoelectric fiber composites

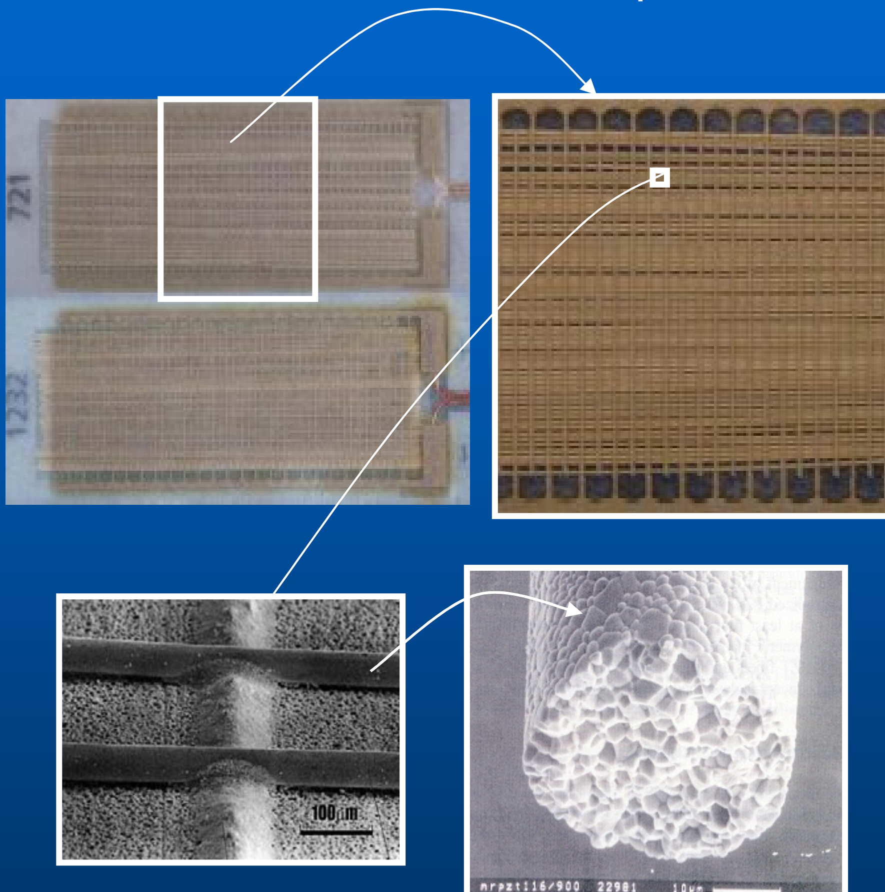

FhG's Würzburg, Dresden, Bremen

Piezoelectric fibres

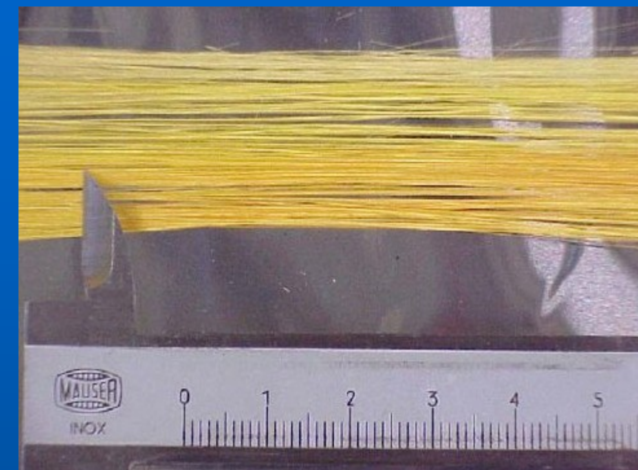

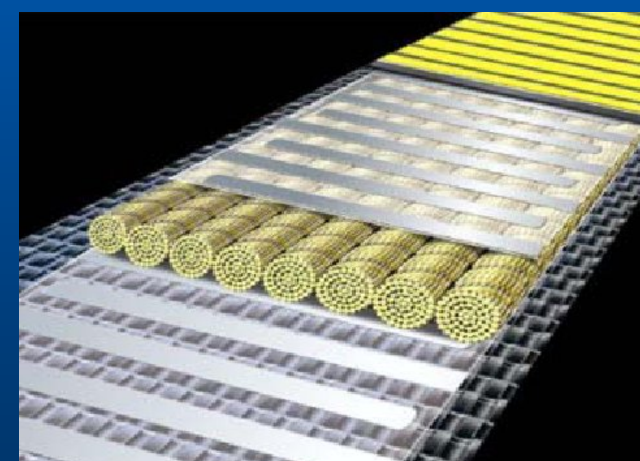

Draft of a piezoelectric fiber composite

$$\begin{Bmatrix} \bar{T}_{11} \\ \bar{T}_{22} \\ \bar{T}_{33} \\ \bar{T}_{23} \\ \bar{T}_{31} \\ \bar{T}_{12} \\ \bar{D}_{1} \\ \bar{D}_{2} \\ \bar{D}_{3} \end{Bmatrix} = \begin{bmatrix} C_{11}^{eff} & C_{12}^{eff} & C_{13}^{eff} & 0 & 0 & 0 & 0 & 0 & -e_{13}^{eff} \\ C_{12}^{eff} & C_{11}^{eff} & C_{13}^{eff} & 0 & 0 & 0 & 0 & 0 & -e_{13}^{eff} \\ C_{13}^{eff} & C_{13}^{eff} & C_{33}^{eff} & 0 & 0 & 0 & 0 & 0 & -e_{33}^{eff} \\ 0 & 0 & 0 & C_{44}^{eff} & 0 & 0 & 0 & -e_{15}^{eff} & 0 \\ 0 & 0 & 0 & 0 & C_{44}^{eff} & 0 & -e_{15}^{eff} & 0 & 0 \\ 0 & 0 & 0 & 0 & 0 & C_{66}^{eff} & 0 & 0 & 0 \\ 0 & 0 & 0 & 0 & e_{15}^{eff} & 0 & \varepsilon_{11}^{eff} & 0 & 0 \\ 0 & 0 & 0 & e_{15}^{eff} & 0 & 0 & 0 & \varepsilon_{11}^{eff} & 0 \\ e_{13}^{eff} & e_{13}^{eff} & e_{33}^{eff} & 0 & 0 & 0 & 0 & 0 & \varepsilon_{33}^{eff} \end{bmatrix} \begin{Bmatrix} \bar{S}_{11} \\ \bar{S}_{22} \\ \bar{S}_{33} \\ \bar{S}_{23} \\ \bar{S}_{31} \\ \bar{S}_{12} \\ \bar{E}_{1} \\ \bar{E}_{2} \\ \bar{E}_{3} \end{Bmatrix}$$

zero values due to choosen bound. conditiones

1. Using the third row to calculate C_{33}^{eff}

$$\bar{T}_{33} = C_{33}^{eff}\,\bar{S}_{33} \longrightarrow \boxed{C_{33}^{eff} = \bar{T}_{33} / \bar{S}_{33}}$$

2. Using the first row: to calculate C_{13}^{eff}

$$\bar{T}_{11} = C_{13}^{eff}\,\bar{S}_{33} \longrightarrow \boxed{C_{13}^{eff} = \bar{T}_{11} / \bar{S}_{33}}$$

Example

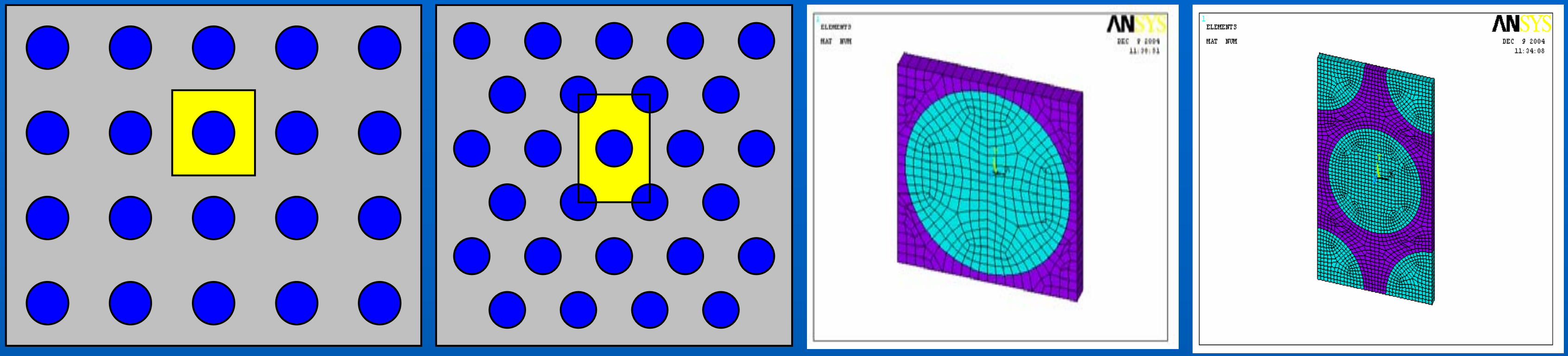

Piezoelectric fibres made from PZT 5A (N/m², C/m² and F/m)

	C11 * E10	C 12* E10	C 13 * E10	C 33 * E10	C 44 * E10
PZT	12.1	7.54	7.52	11.1	2.11
	e15	**e31**	**e33**	**ε11 * E-9**	**ε33* E-9**
PZT	12.3	-5.4	15.8	8.11	7.35

Matrixmaterial: Polymermaterial with E=1.806 E9 N/m², ν= 0.3994

Fibre volume fraction

0.111 0.222 0.333 0.444 0.556 0.667

Example: Results

Selected results compared with calculations based on other methods

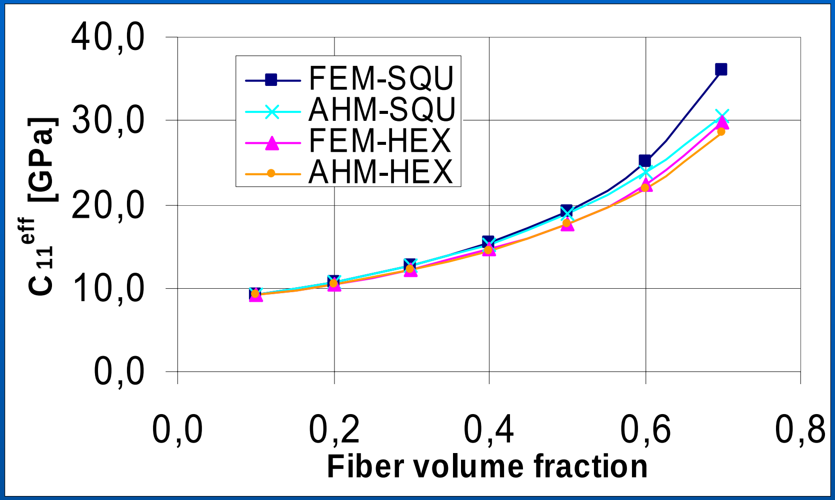

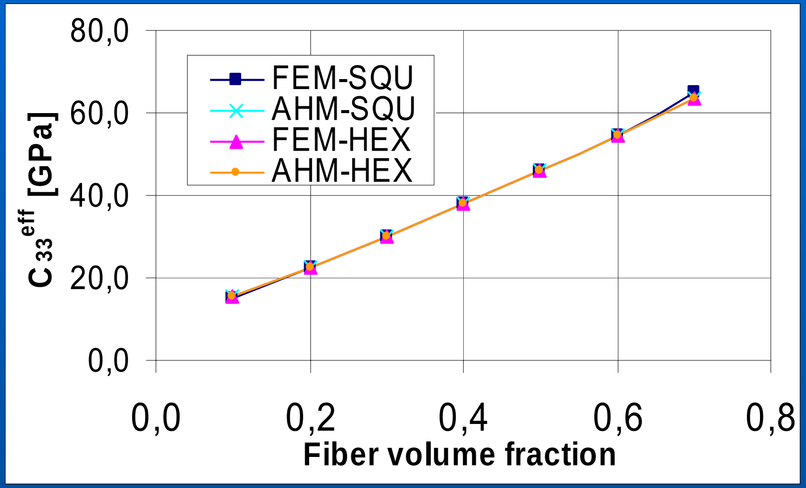

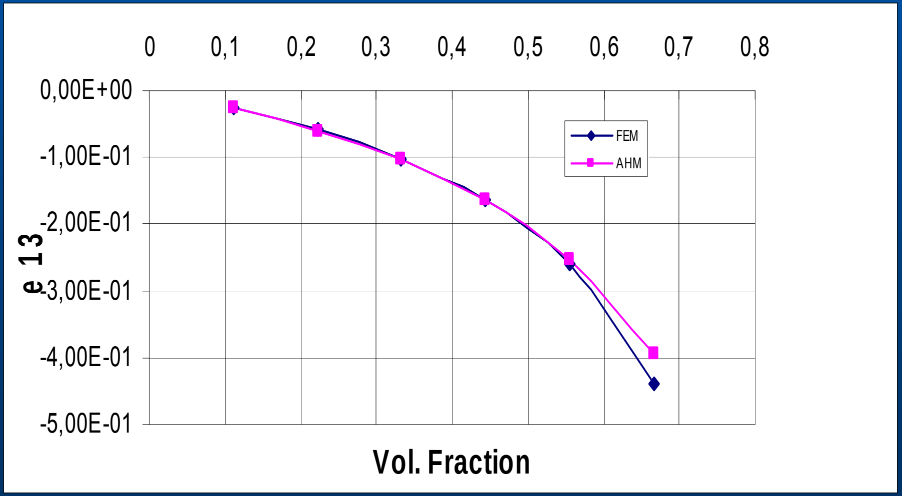

Shell type models for piezoelectric composites

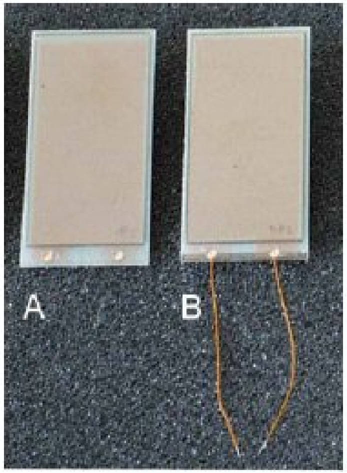

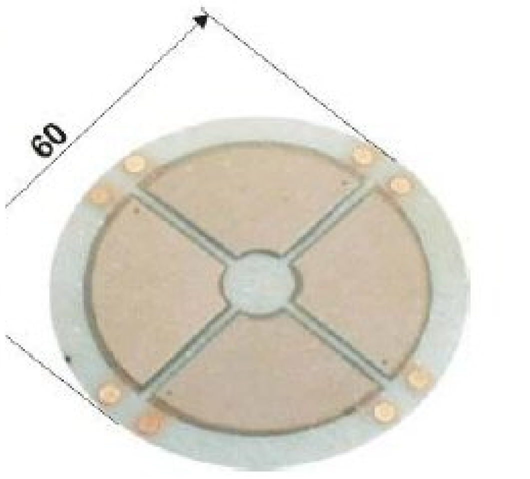

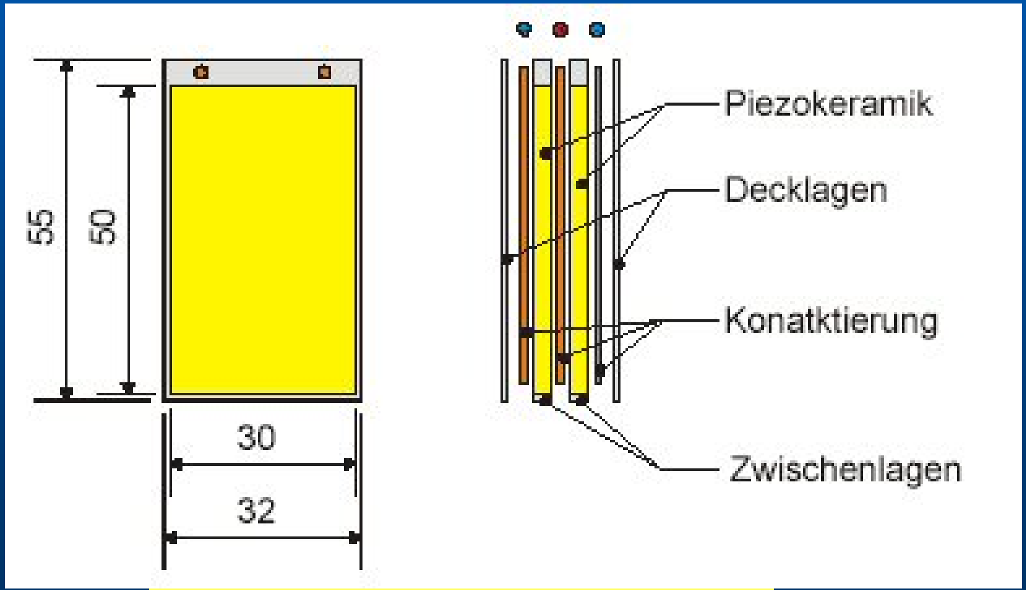

Modelling of piezoelectric composites based on CLT

Classical SemiLoof shell element

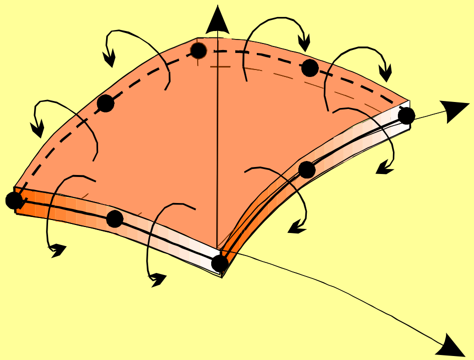

Quadrilateral element with 32 dof's

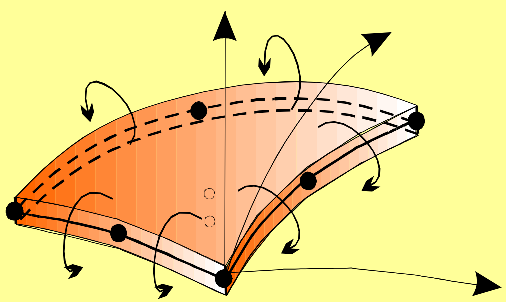

Triangular element with 24 dof's

- Basis: Discrete-Kirchhoff Theory (DKT)
- *Lagrangian* and *Legendre* polynomials
- Tangential rotations only

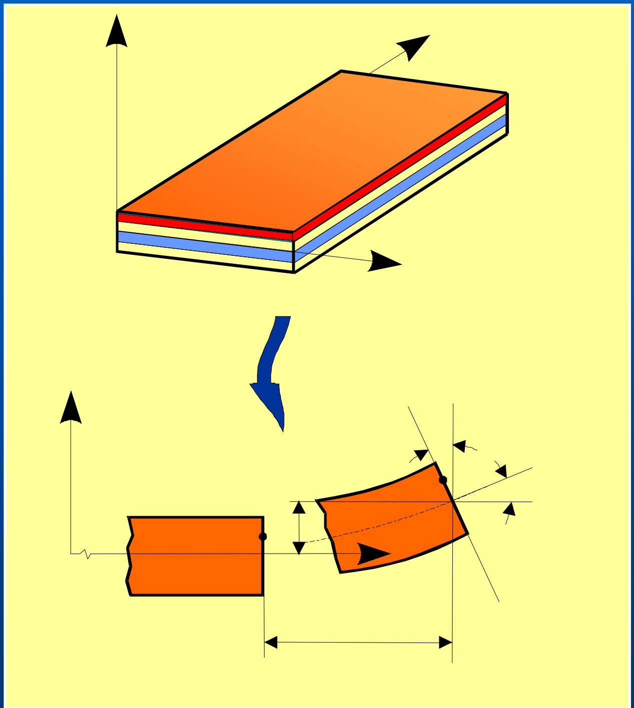

Extension to an active piezoelectric composite shell element

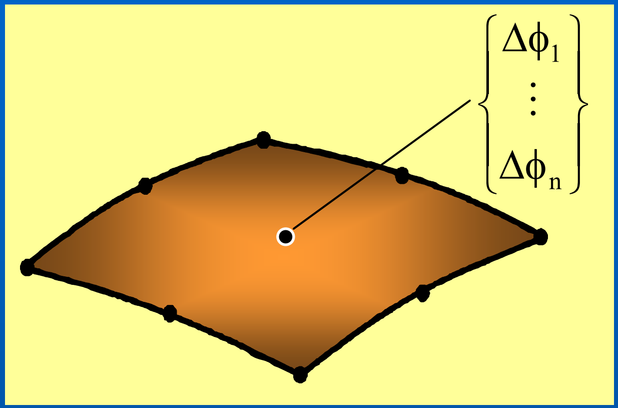

- Electromechanical coupling is taken into account
- The piezoelectric layers are assumed to be complete metalized and electrodized, where the electric field E_{3i} is again assumed to be constant over thickness h_i:

$$E_{3i}=\Delta\phi/h$$

- The element is enhanced by additional electric potential differences $\Delta\phi_i$ for each active layer *i.* The coupling is taken into account by:

$$\begin{bmatrix} \mathbf{K}_e^{(mm)} & \mathbf{K}_e^{(me)} \\ \mathbf{K}_e^{(me)^T} & \mathbf{K}_e^{(ee)} \end{bmatrix} \begin{Bmatrix} \mathbf{u}_e \\ \Delta\boldsymbol{\varphi}_e \end{Bmatrix} = \begin{Bmatrix} \mathbf{f}_e^{(m)} \\ \mathbf{f}_e^{(e)} \end{Bmatrix}$$

$$\mathbf{K}_e^{(mm)} = \int_{A_e} \mathbf{B}^{(m)^T} \mathbf{C}\,\mathbf{B}^{(m)} dA \;;\; \mathbf{K}_e^{(me)} = \int_{A_e} \mathbf{B}^{(m)^T} \mathbf{e}\,\mathbf{B}^{(e)} dA \;;\; \mathbf{K}_e^{(ee)} = \int_{A_e} \mathbf{B}^{(e)^T} \boldsymbol{\kappa}\,\mathbf{B}^{(e)} dA$$

The assumption of the electric field has been intensively investigated!

Controller design

$$\mathbf{M}\ddot{\mathbf{q}} + \mathbf{D}_d\dot{\mathbf{q}} + \mathbf{K}\mathbf{q} = \overline{\mathbf{E}}\mathbf{f}(t) + \overline{\mathbf{B}}\mathbf{u}(t)$$

Model reduction (e.g. modal space): $\mathbf{q} = \mathbf{\Phi}\mathbf{z}$

State space representation: $\mathbf{x}^{\mathrm{T}} = [\mathbf{z} \quad \dot{\mathbf{z}}]^{\mathrm{T}}$

$$\dot{\mathbf{x}}(t) = \begin{bmatrix} \mathbf{0} & \mathbf{I} \\ -\mathbf{\Lambda}_r & -\mathbf{\Lambda}_r \end{bmatrix} \mathbf{x}(t) + \begin{bmatrix} \mathbf{0} \\ \mathbf{\Phi}_r^{\mathrm{T}}\overline{\mathbf{B}} \end{bmatrix} \mathbf{u}(t) + \begin{bmatrix} \mathbf{0} \\ \mathbf{\Phi}_r^{\mathrm{T}}\overline{\mathbf{E}} \end{bmatrix} \mathbf{f}(t)$$

$$\dot{\mathbf{x}} = \mathbf{A}\mathbf{x} + \mathbf{B}\mathbf{u} + \mathbf{E}\mathbf{f}$$
$$\mathbf{y} = \mathbf{C}\mathbf{x} + \mathbf{D}\mathbf{u} + \mathbf{F}\mathbf{f}$$

Data exchange FEA and controller design software

FE system COSAR

$$\mathbf{M}\ddot{\mathbf{q}}+\mathbf{D}_d\,\dot{\mathbf{q}}+\mathbf{K}\mathbf{q}=\bar{\mathbf{E}}\mathbf{f}(t)+\bar{\mathbf{B}}\mathbf{u}(t)$$

Eigenvalue analysis, modal reduction and transformation into the state space form

$$\dot{\mathbf{x}}=\mathbf{A}\mathbf{x}+\mathbf{B}\mathbf{u}(t)+\mathbf{E}\mathbf{f}(t)$$
$$\mathbf{y}=\mathbf{C}\mathbf{x}+\mathbf{D}\mathbf{u}(t)+\mathbf{F}\mathbf{f}(t)$$

FE / control interface

Modal state space matrices
A, B, C, D, E, F

Controller matrix
L

Matlab/Simulink

Controller design

$\mathbf{u}(t) = -\mathbf{L}\mathbf{x}$

LQ-Controller with observer and additional dynamics

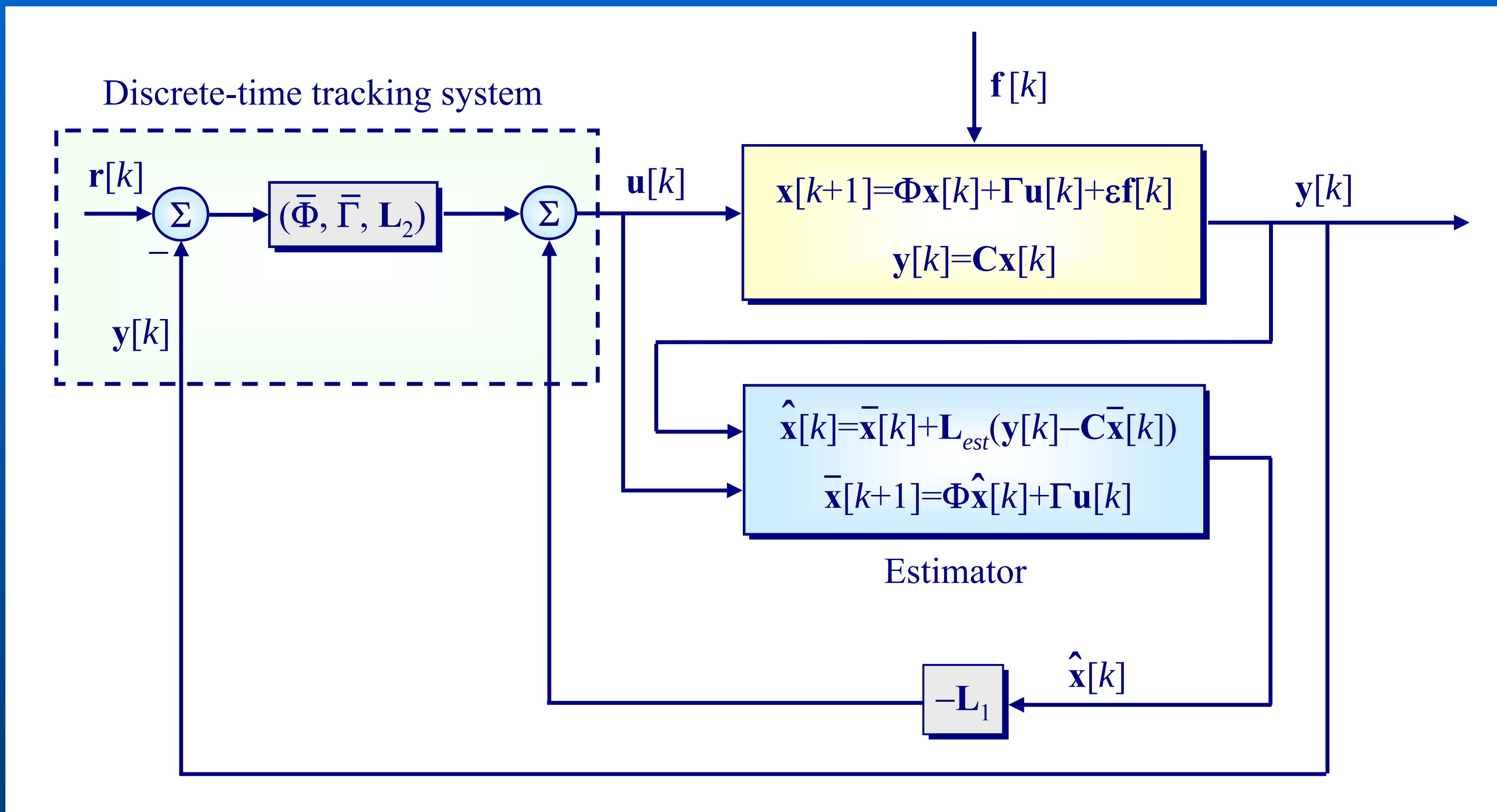

see: T. Nestorović, PhD thesis, Uni Magdeburg, VDI Düsseldorf, 2005

Best positions of actuators/sensors at structures

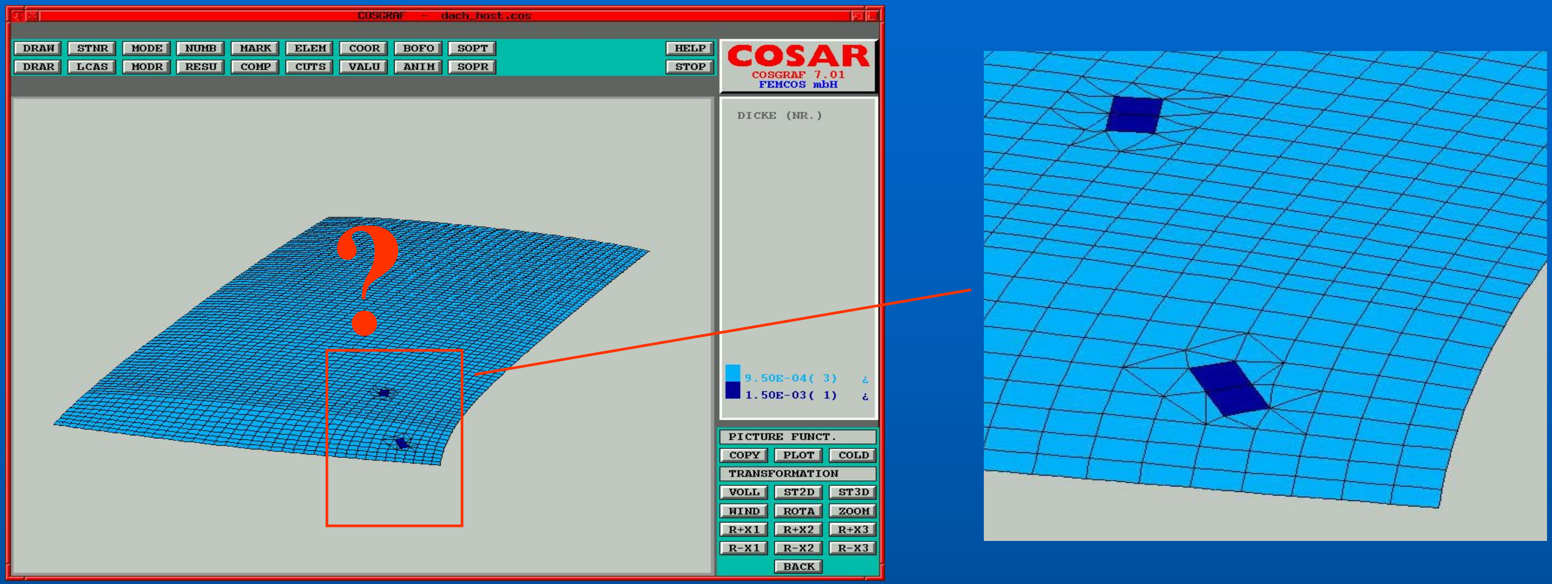

I) **Discrete continuous optimization (gradient based methods)**
[see the Weber/Gabbert (1998,99); Schulz/Gabbert(2001)]

II) **Controllability and observeability index**
[see Seeger/Köppe/Gabbert (2002)]

III) **Continuous optimization (gradient based methods)**
[see Seeger/Gabbert (2003)]

IV) **Evolutionary optimization**
[see Bohn/Gabbert (2004), WCCM VI]

Automatic integration of a patch mesh in a base mesh

- Projection of the FE-mesh of the piezoelectric patch into the host structure
- Identification of overlapping elements
- Local remeshing of the host structure with embedded piezoelectric patch

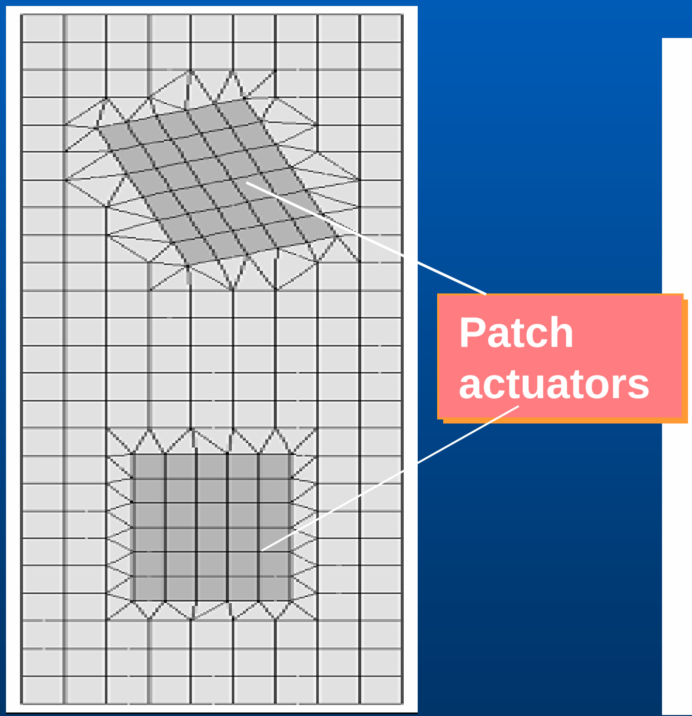

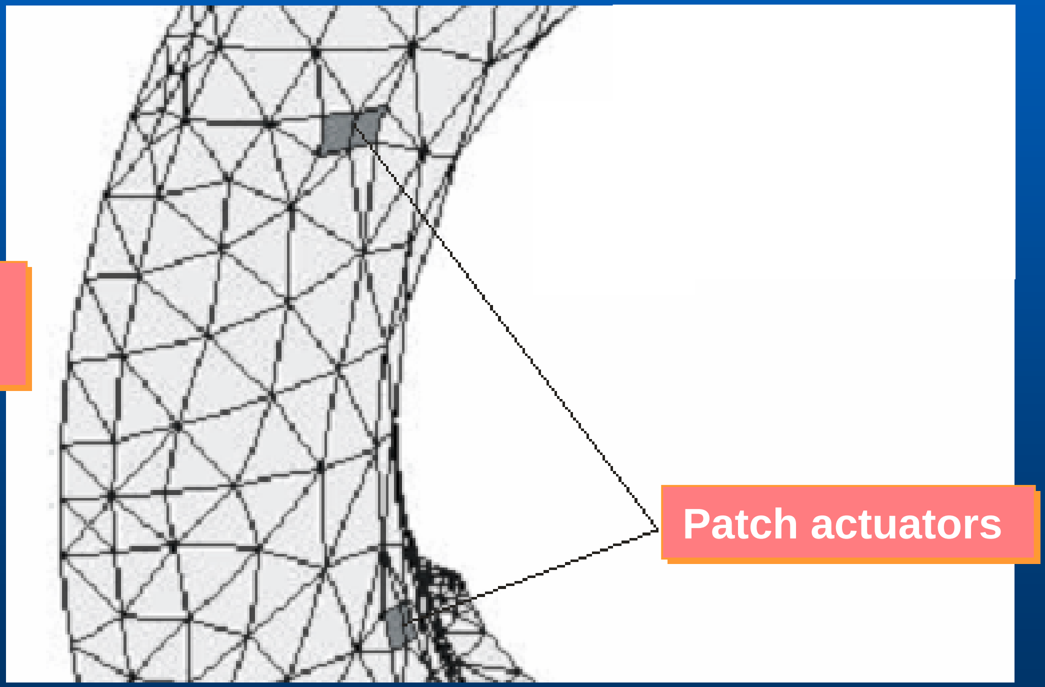

Accuracy of the model for gradient based optimization

Sensitivity

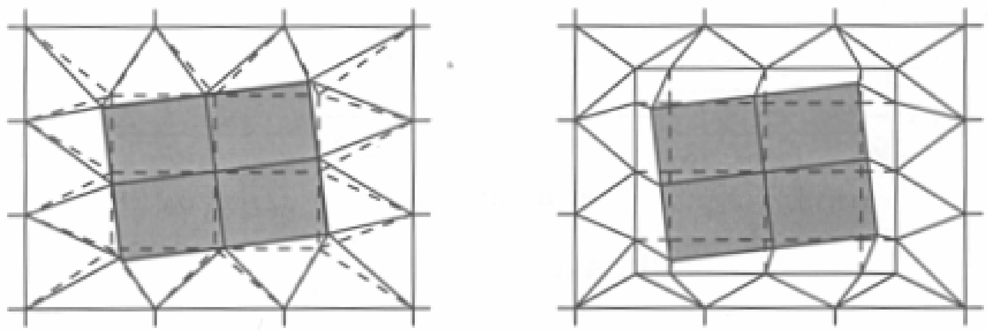

(a) (b)

Accuracy

Objective function: accuracy sufficient with mesh a) and b)

Gradients: accuracy not sufficient with mesh a)

accuracy sufficient with mesh b)

see: F. Seeger, PhD thesis, Uni Magdeburg, VDI Düsseldorf, 2004

Gradient based optimisation in the frequency domain

Starting point is the state space formulation

$$\dot{\mathbf{z}}(t)=\begin{bmatrix}\mathbf{0} & \mathbf{I}\\ -\boldsymbol{\Lambda} & -\boldsymbol{\Delta}\end{bmatrix}\mathbf{z}(t)+\begin{bmatrix}\mathbf{0}\\ \boldsymbol{\Phi}^T\mathbf{B}\end{bmatrix}\mathbf{u}(t)+\begin{bmatrix}\mathbf{0}\\ \boldsymbol{\Phi}^T\mathbf{E}\end{bmatrix}\mathbf{f}(t)=\mathbf{A}\mathbf{z}+\mathbf{B}\mathbf{u}(t)+\mathbf{E}\mathbf{f}(t)$$

$$\mathbf{y}=\mathbf{C}\mathbf{z}$$

Transformation in the frequency domain results in

$$j\omega\mathbf{Z}(j\omega)=\mathbf{A}\mathbf{Z}(j\omega)+\mathbf{B}\mathbf{U}(j\omega)+\mathbf{E}\mathbf{F}(j\omega)$$
$$\mathbf{Y}(j\omega)=\mathbf{C}\mathbf{Z}(j\omega)$$

Introducing a controller in the form of $\mathbf{U}(j\omega)=-\mathbf{K}\,\mathbf{Z}(j\omega)$ results in

$$\mathbf{Y}(j\omega)=\underbrace{\mathbf{C}(j\omega\mathbf{I}-\mathbf{A}+\mathbf{B}\mathbf{K})^{-1}\mathbf{E}}_{\mathbf{H}(j\omega)}\mathbf{F}(j\omega)$$
$$=\mathbf{H}(j\omega)\mathbf{F}(j\omega)$$

Gradient based optimisation

The transfer function can be calculated by solving the linear system of equations

$$(j\omega\mathbf{I}-\mathbf{A}+\mathbf{BK})\hat{\mathbf{Z}}(j\omega)=\mathbf{E}$$

$$\mathbf{H}(j\omega)=\mathbf{C}\hat{\mathbf{Z}}(j\omega)$$

For the optimization based on the frequency response function an objective function can be created, such as

$$J_F=\frac{1}{\omega_b-\omega_a}\int_{\omega_a}^{\omega_b}\|\mathbf{H}\|_2^2\,d\omega.$$

In the gradient based optimization the gradients are required:

$$\frac{\partial J_F^c}{\partial p}=\frac{1}{\omega_b-\omega_a}\int_{\omega_a}^{\omega_b}\frac{\partial}{\partial p}\|\mathbf{H}\|_2^2\,d\omega$$

$$\frac{\partial\mathbf{H}}{\partial p}=\frac{\partial\mathbf{C}}{\partial p}\hat{\mathbf{Z}}+\mathbf{C}\frac{\partial\hat{\mathbf{Z}}}{\partial p}.$$

Test example: Optimal actuator and sensor positioning

Clamped plate:
Two actuators to controlling the eigenmodes in a given frequency band

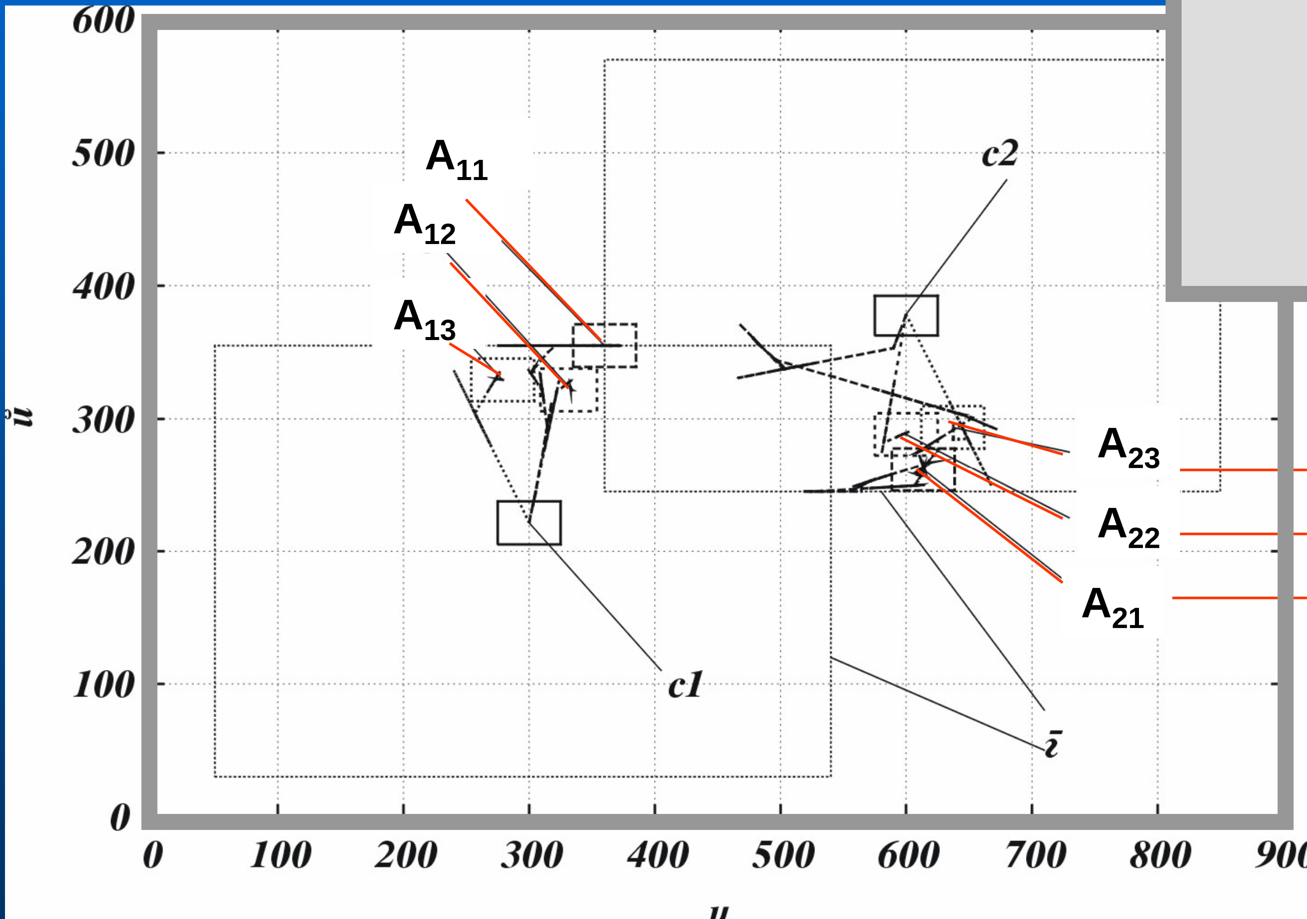

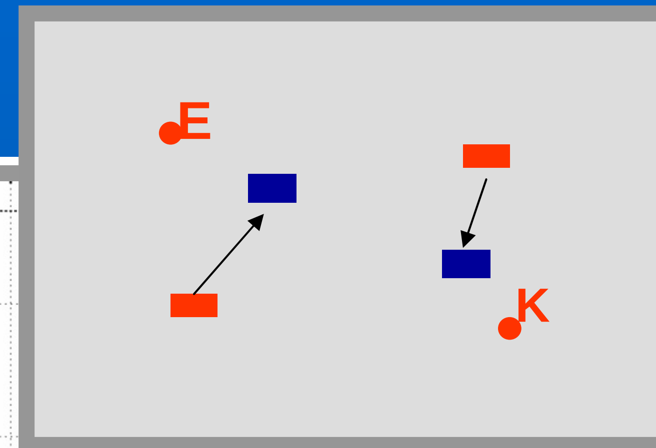

3: 275-325 Hz

2: 150-350 Hz

1: 0-600 Hz

Test example: Results

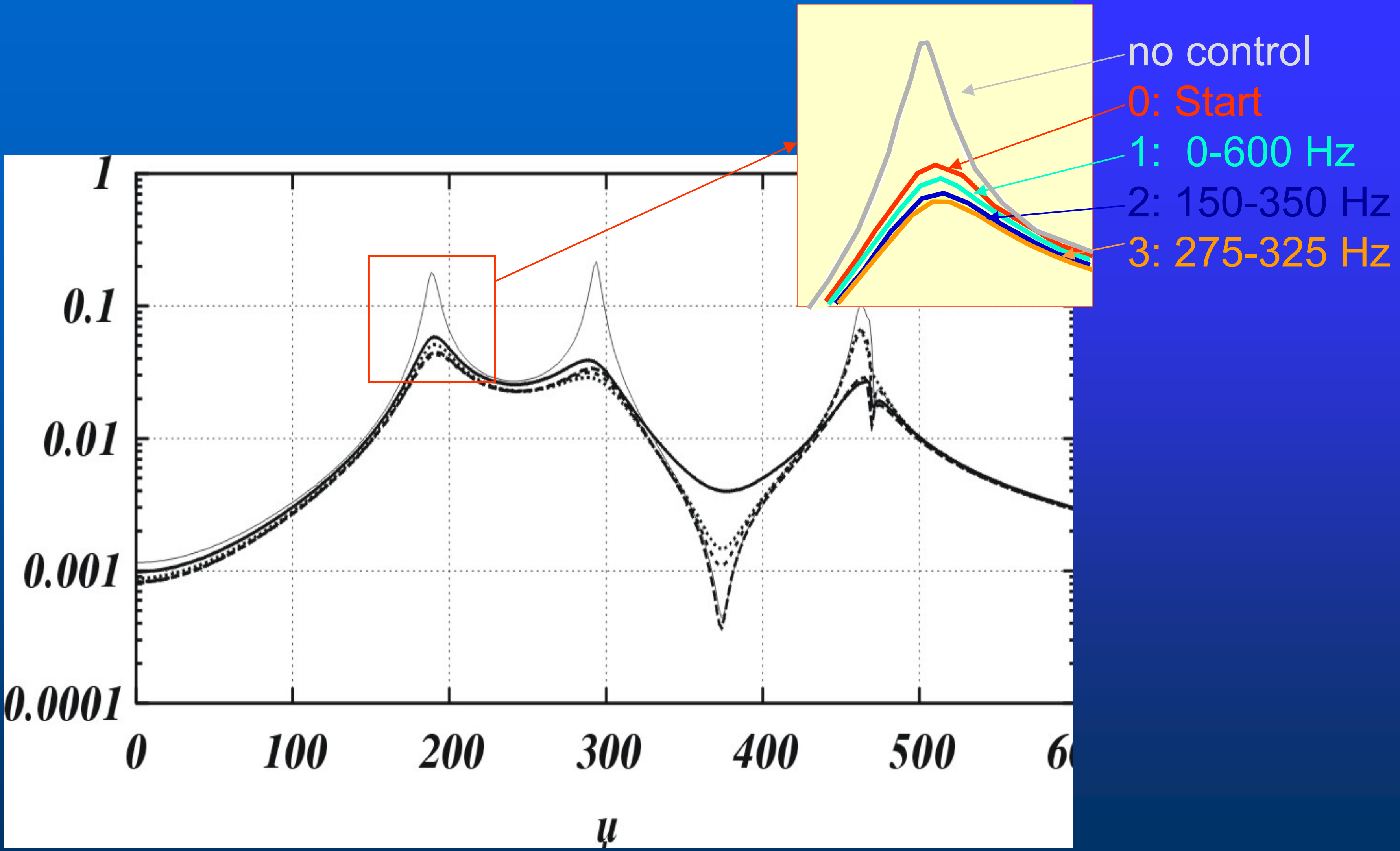

Placement based on a simple criterion

Modal Controllability Index

$$\mu_k = \boldsymbol{\varphi}_k^T \overline{\mathbf{B}}\, \overline{\mathbf{B}}^T \boldsymbol{\varphi}_k$$

This index can be quite simple evaluated based on a finite element model. It can be seen as the signal (voltage of a patch actuator at one point of the mesh, if the structure is excited in one eigenmode). For one mesh point *i* and the k^{th} eigenmode we receive:

$$\mu_{ki} = \varphi_{ki}^2$$

Example 3: Clamped plate

Modal controllability indices of the first five modes of a rectangular clamped plate

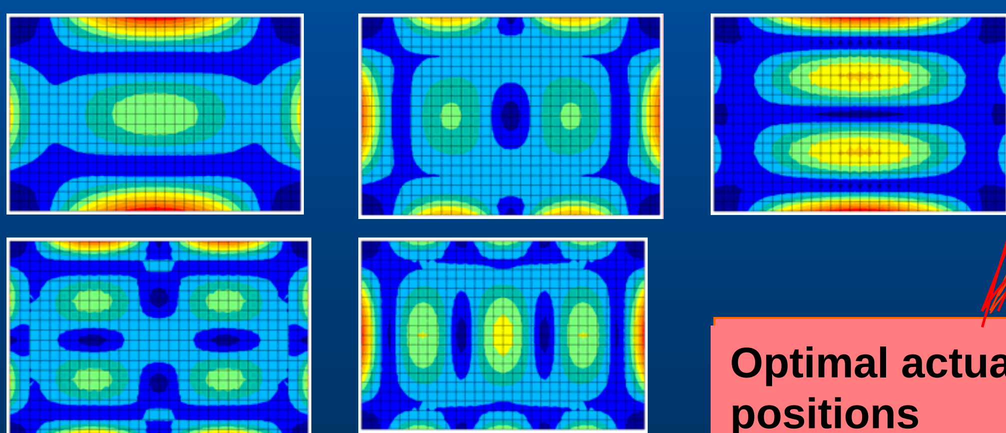

Optimal actuator positions

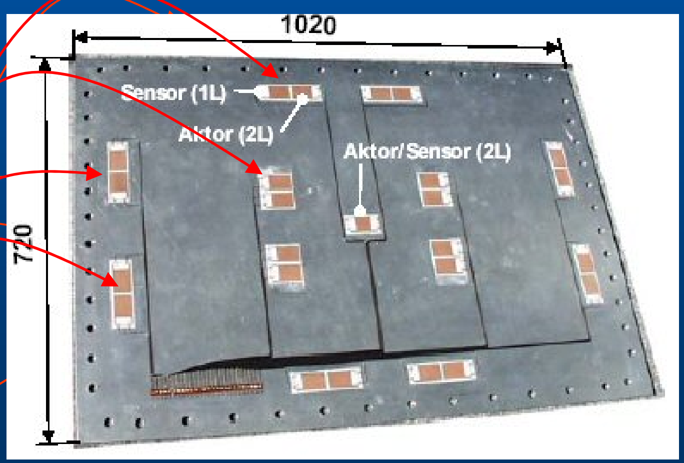

Test example 3: Experimental setup

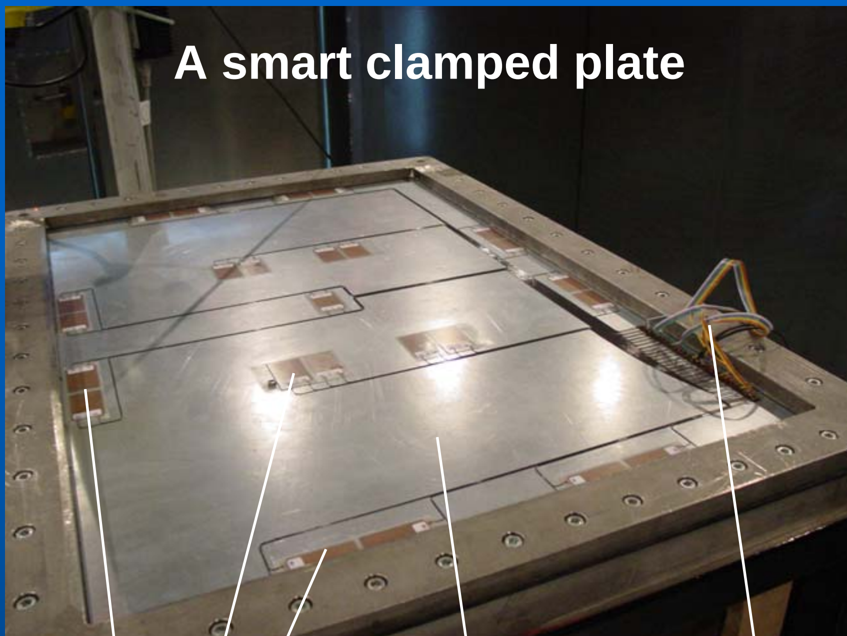

Thin plate made of Al
(or steel, or GFC)

Thin ceramic patches made of PZT

Connection between the ceramic patches and the control unit

Test example: Measurement, impulse excitation and LQ-controller

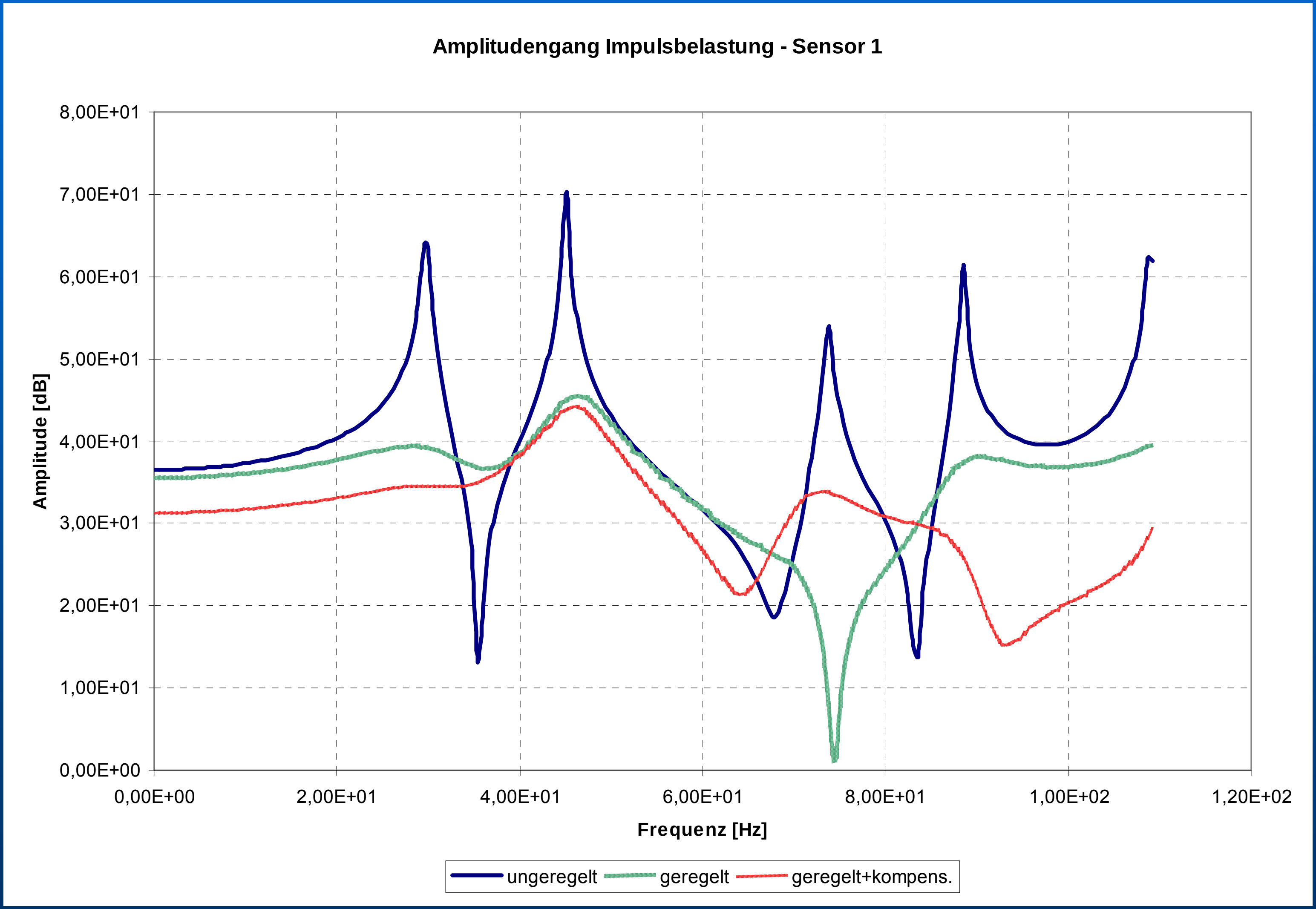

Test example: Optimal angel of patch actuator

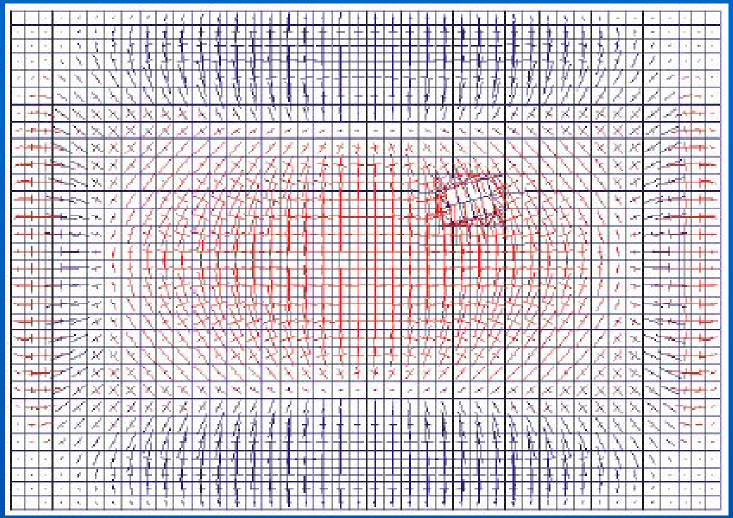

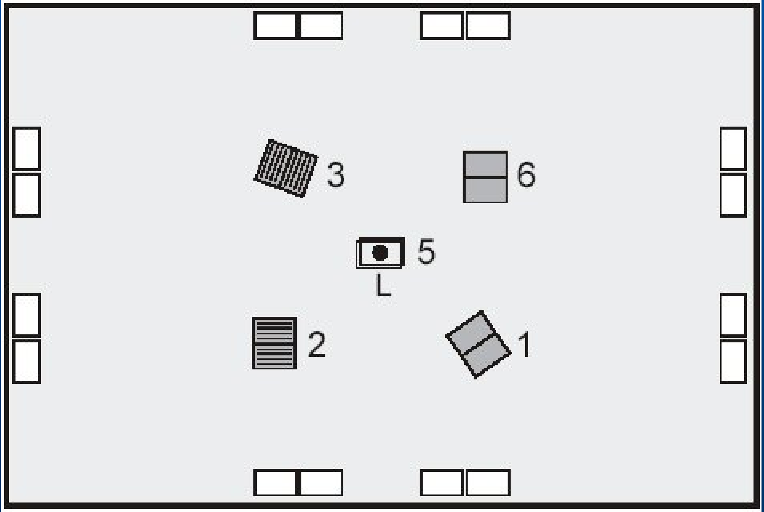

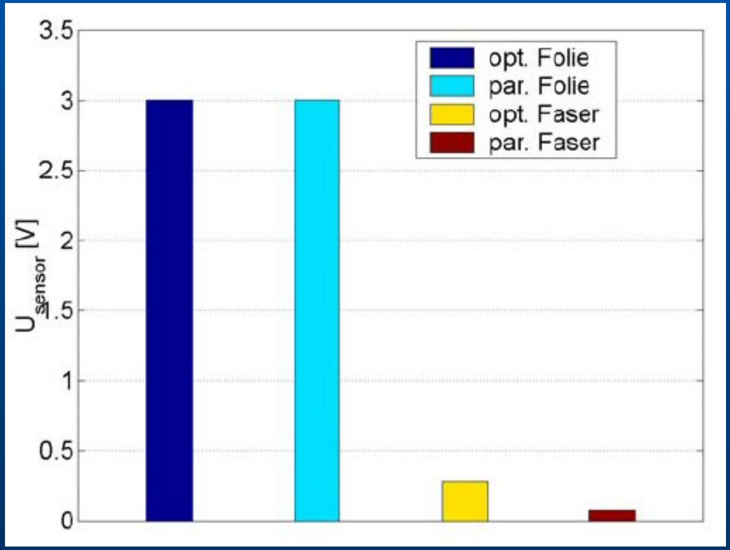

Test example: Acoustic box

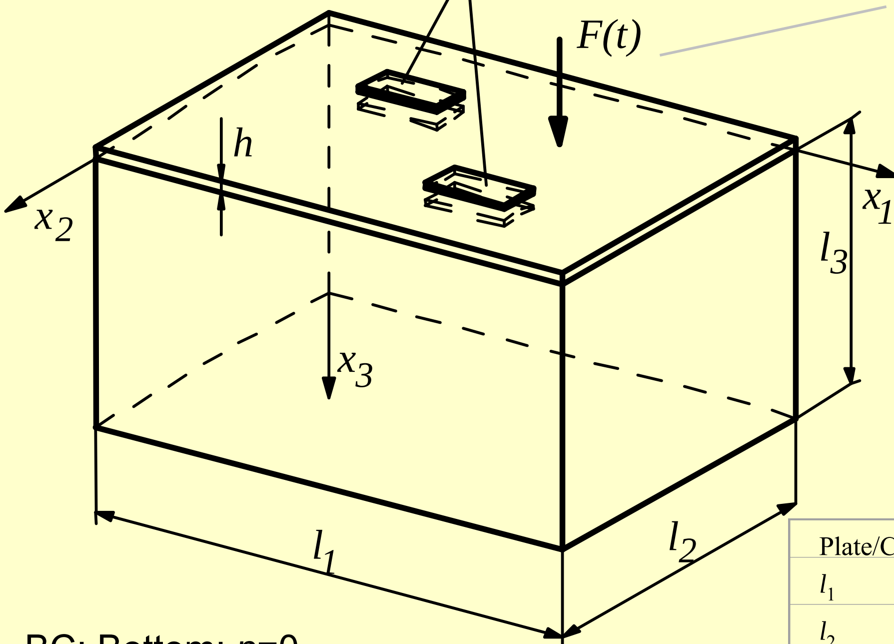

Excitation with a sin-signal containing the first two eigenfrequencies of the system

Young's modulus E	210000N/mm²
Poisson's ratio ν	0.3
Density ρ_P	$2.63\cdot10^{-9}$Ns²/mm⁴

Speed of sound c	340000mm/s
Fluid density ρ_0	$1.29\cdot10^{-12}$Ns²/mm⁴

BC: Bottom: p=0
Sidewalls: v=0

Plate/Cavity System		Actuators/Sensors	
l_1	600mm	Length in x_1-direction	100mm
l_2	400mm	Length in x_2-direction	50mm
l_3	400mm	Patch thickness	0.2mm
h (Plate thickness)	2mm		

Elastic Constants				Piezoelectric Constants		Dielectric Constants	
c_{11}	107600N/mm²	c_{33}	100400N/mm²	e_{15}	$1.20\cdot10^{-5}$N/(mV)mm	κ_{11}	$1.74\cdot10^{-14}$N/(mV)²
c_{12}	63120N/mm²	c_{44}	19620N/mm²	e_{31}	$-9.60\cdot10^{-6}$N/(mV)mm	κ_{33}	$1.87\cdot10^{-14}$N/(mV)²
c_{13}	63850N/mm²	c_{66}	22200N/mm²	e_{33}	$1.51\cdot10^{-5}$N/(mV)mm	Density ρ	$7.80\cdot10^{-9}$Ns²/mm⁴

Test example: Acoustic box, results

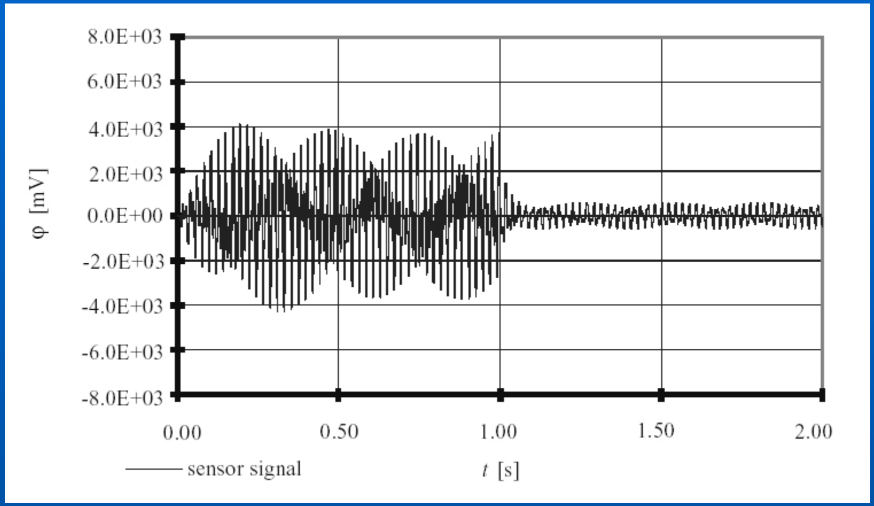

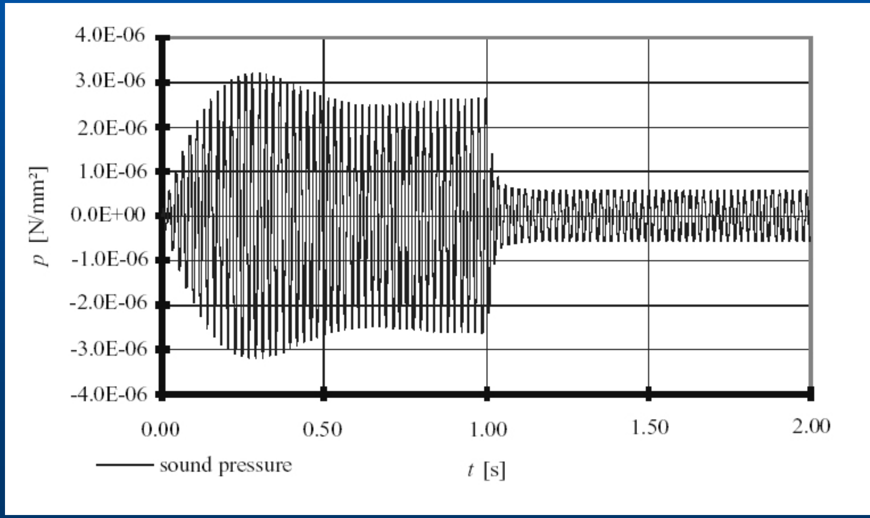

Industrial example: Active vibration control of a MRT

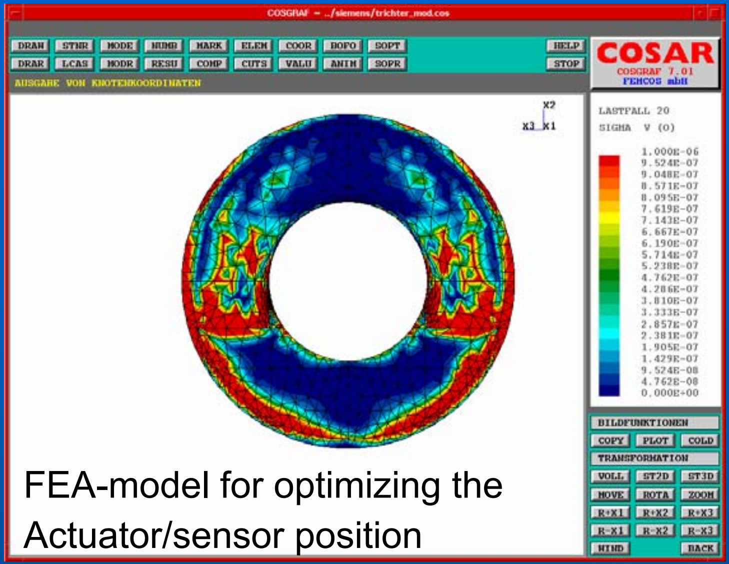

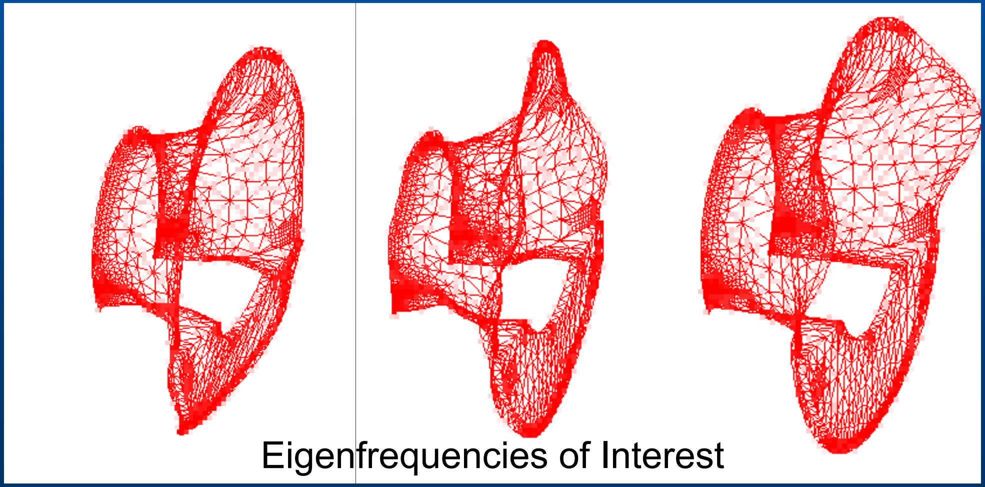

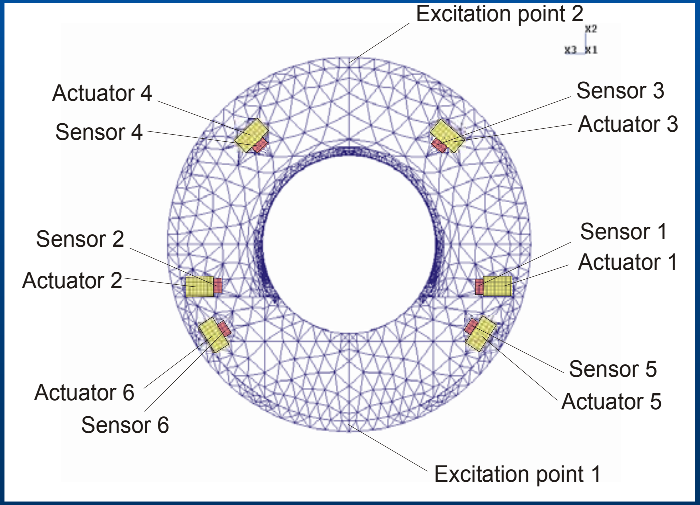

Active vibration reduction of a funnel of a MRT

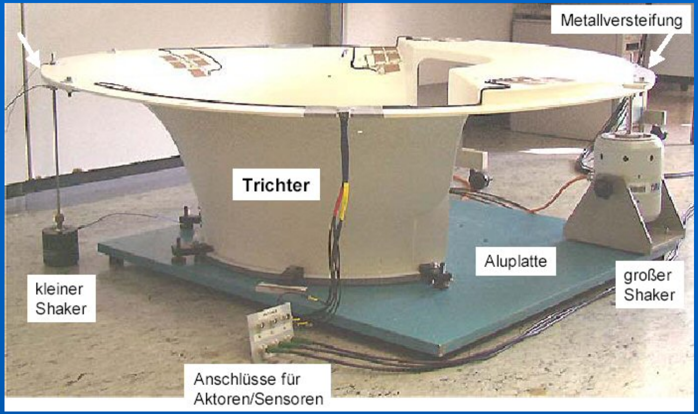

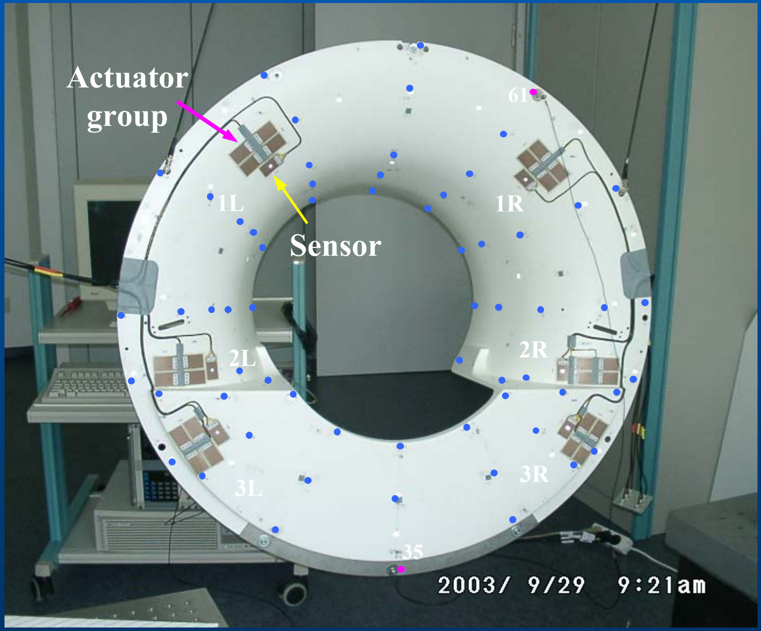

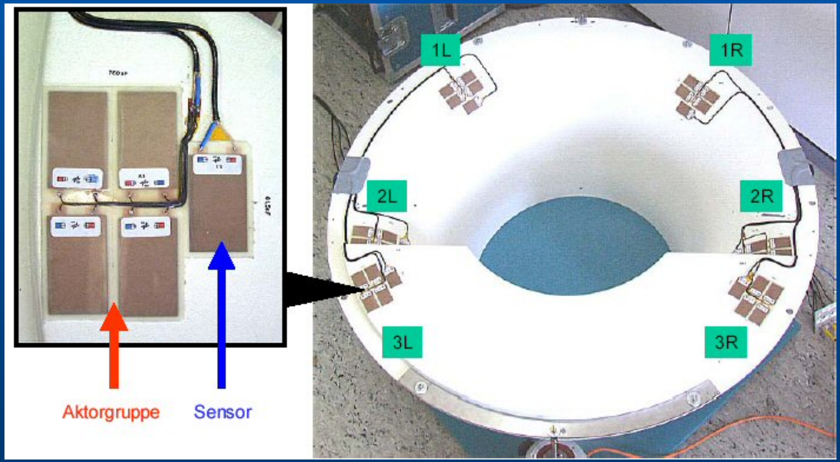

Active vibration reduction of a funnel of a MRT

Hardware-in-the-loop experiments

Accelerometer

Experimental rig for the modal analysis
with the funnel and
LMS CADA-X system

The scheme of the funnel experimental rig for the modal analysis

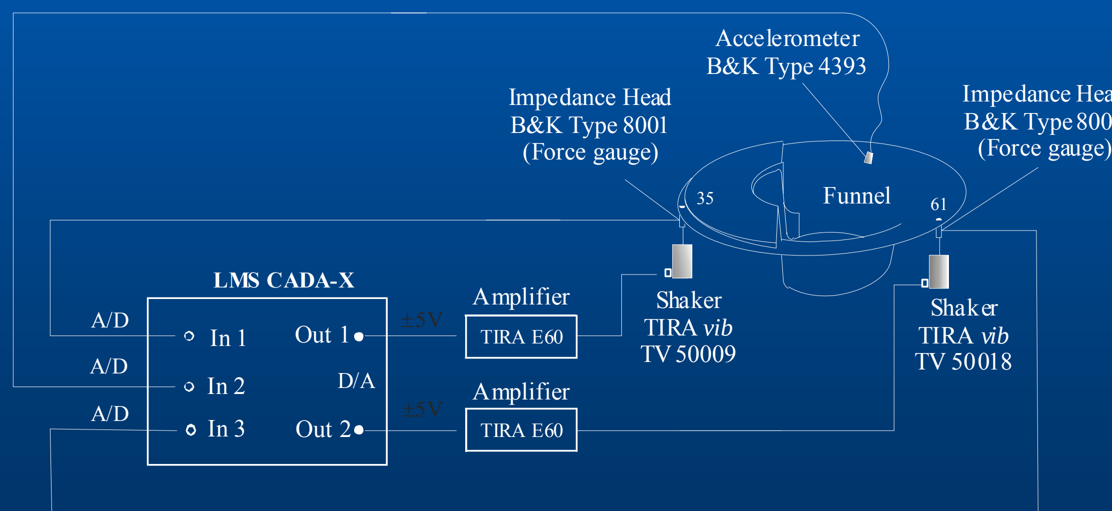

Active vibration reduction of a funnel of a MRT

Measured and identified Frequency Response Functions for actuator/sensor pairs A1R-S1L

A2R-S1R

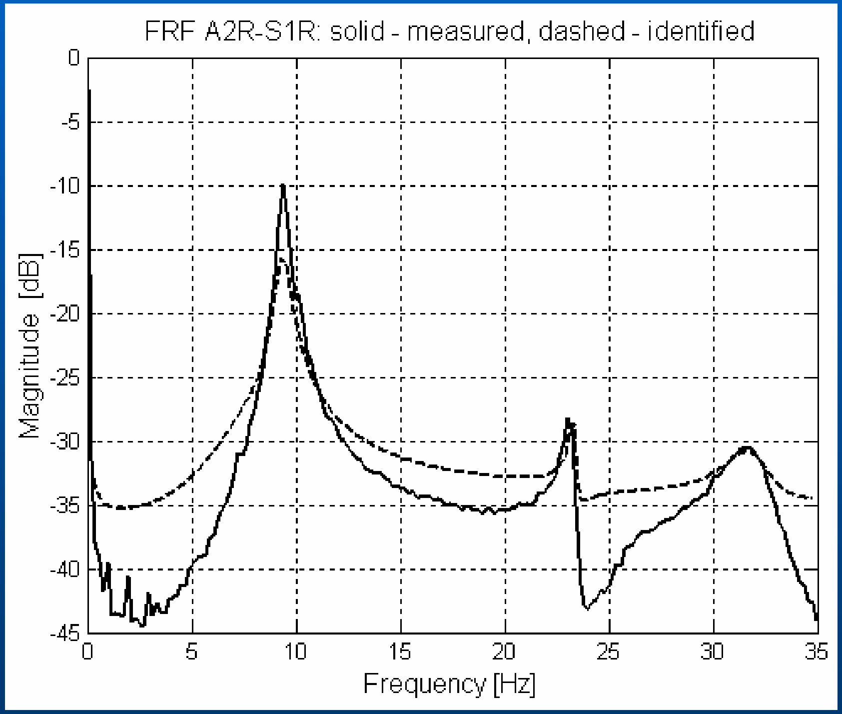

A1R-S1L

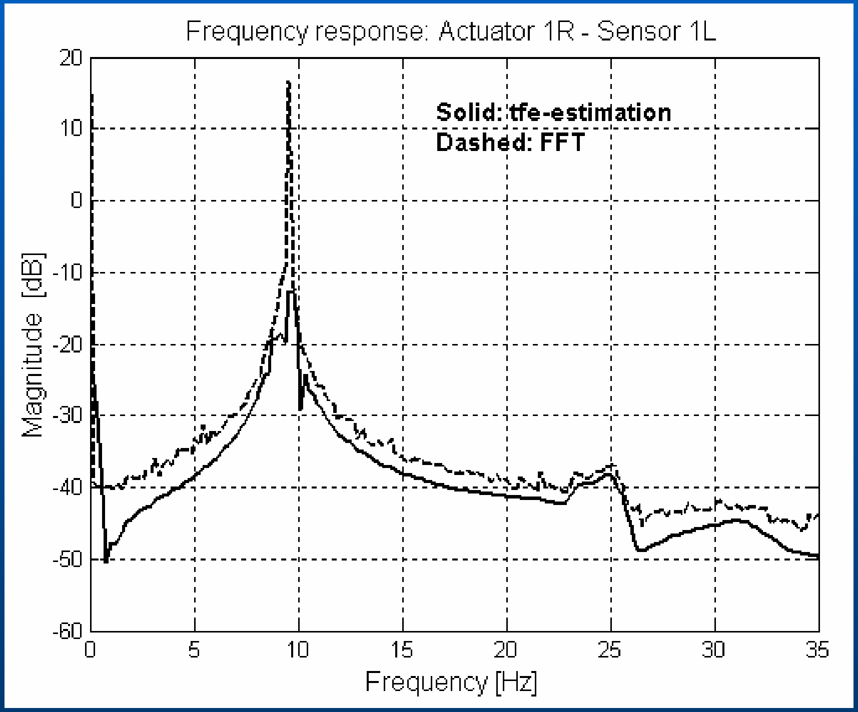

Optimal LQ control

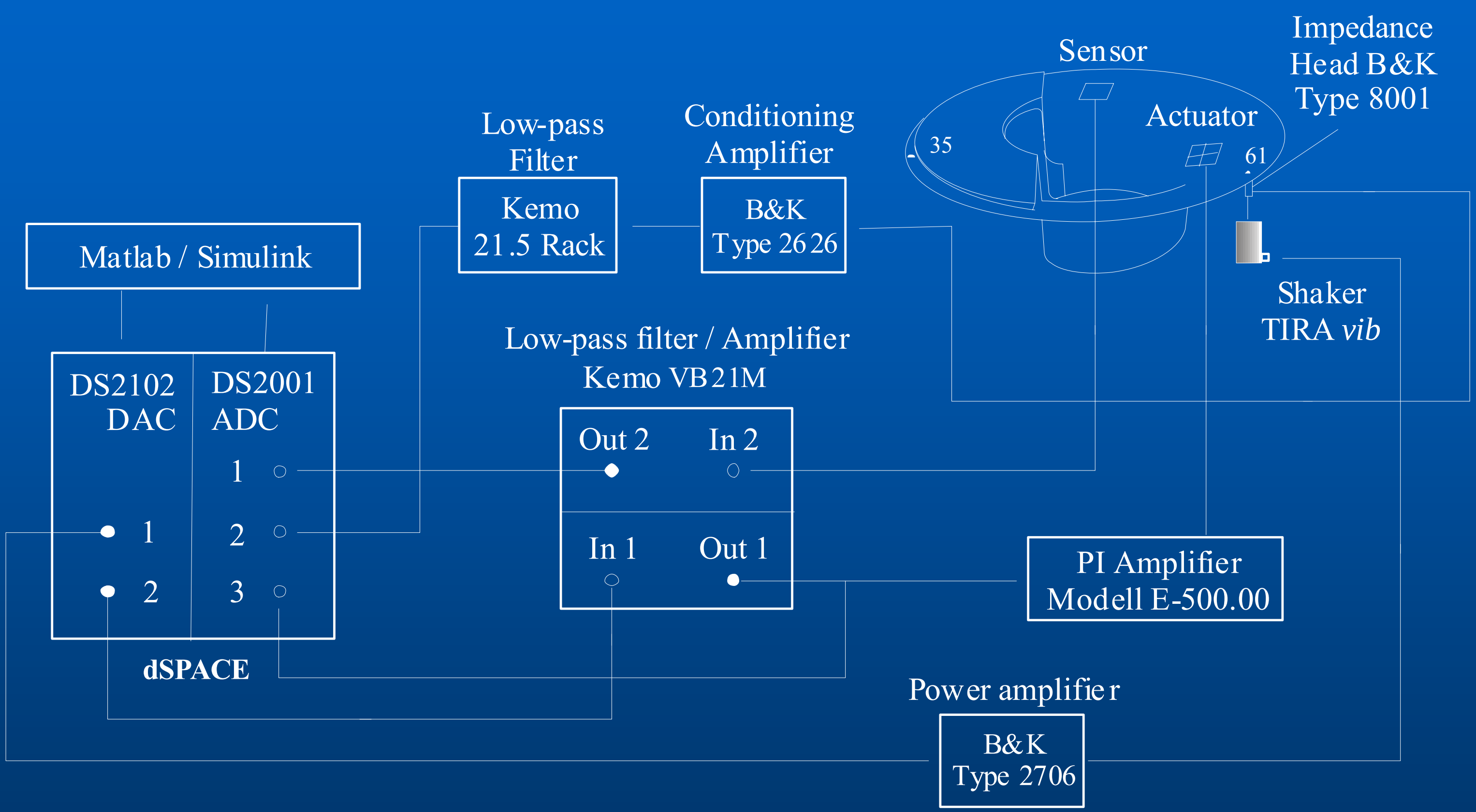

Industrial Example: Control of the first eigenfrequency

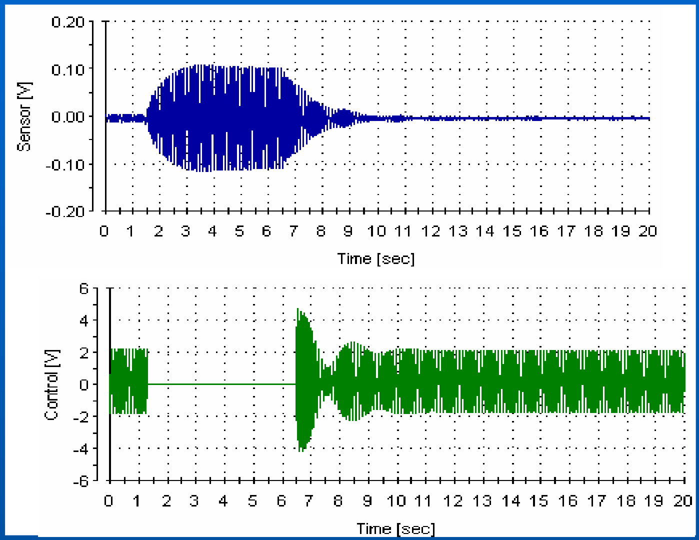

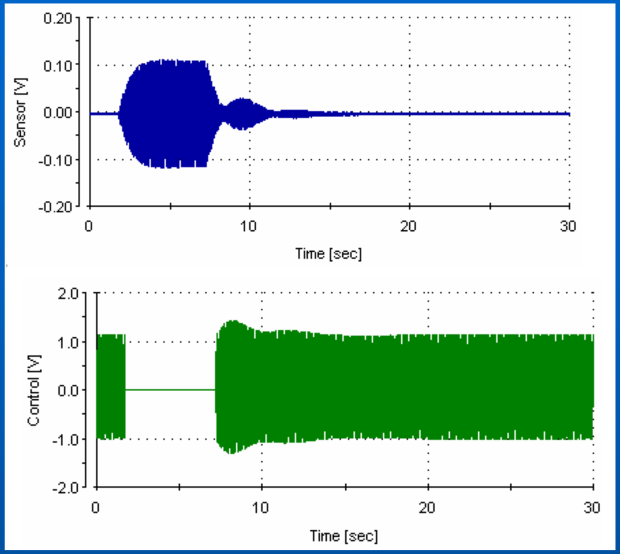

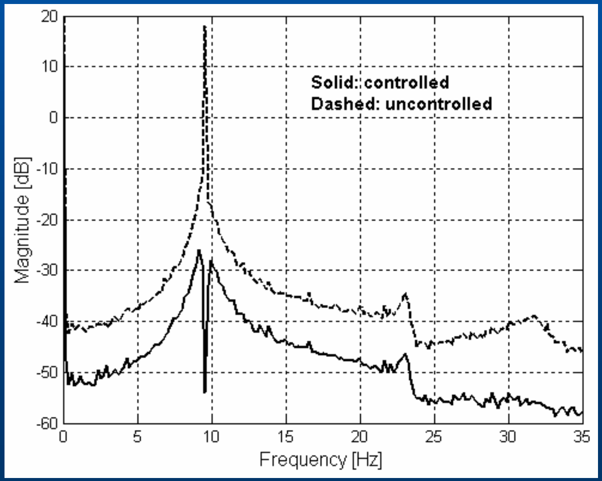

Actuator/sensor pairs A2R–S1R

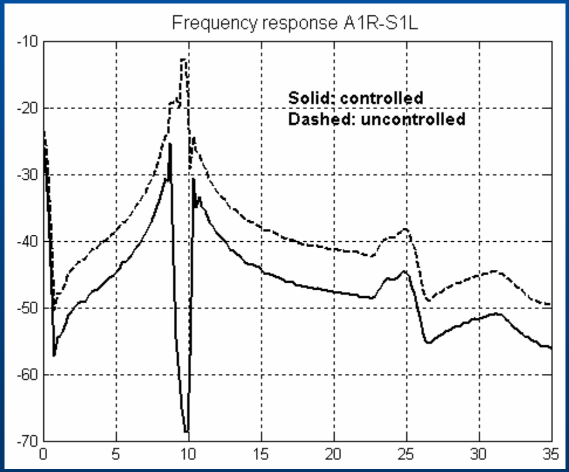

Actuator/sensor pairs A1R–S1L

Summary

- In the presentation it was shown, that an overall virtual development approach to design and to evaluate smart structures concepts is required.
- For smart structures design a finite element approach coupled with controller design software Matlab/Simulink was discussed.
- For piezoelectric fibre composites a homogenisation technique based on a RVE approach to evaluate effective material properties was presented.
- For thin-walled structures shell type finite elements were shown, which are an effective approach for an overall design procedure.
- In controller design we have used model based optimal LQ (FE-model and/or identified model) with Kalman estimator and additional dynamics, which was briefly discussed only.
- For calculating best positions of actuators/sensors at structures a gradient based optimization was presented. But simpler methods based on a modal criterion have shown to result in a first acceptable solution.
- The design procedure was applied to several test cases and industrial applications, where also hardware-in-the-loop realizations have been performed to evaluate the results.
- Recent activities are also focused on smart machine systems, which perform large motion, where as design basis an multi-body systems (MBS) approach is used.